

Searching for substellar companion candidates with *Gaia*

II. A catalog of 9,698 planet candidate solar-type hosts[★]

F. Kiefer¹, A.-M. Lagrange¹, P. Rubini², and F. Philipot¹

¹ LESIA, Observatoire de Paris, Université PSL, CNRS, Sorbonne Université, Université de Paris, 5 place Jules Janssen, 92195 Meudon, France^{**}

² Pixyl, 5 av du Grand Sablon 38700 La Tronche

Received 31/07/2024 ; accepted 03/09/2024

ABSTRACT

Context. In a previous paper, we introduced a new tool called "*Gaia* DR3 proper motion anomaly and astrometric noise excess", or GaiaPMEX. This tool characterizes the mass and semi-major axis relative to the central star (sma) of a possible companion around any source observed with *Gaia* using the value of renormalized unit weight error (ruwe), or with both *Gaia* and HIPPARCOS using the value of the proper motion anomaly (PMA), either alone or combined with the ruwe.

Aims. Our goal is to exploit the large volume of sources in the third *Gaia* data release catalog to find new exoplanet candidates. We wish to create a new input catalog of planet-candidate-hosting systems to enable future follow-up projects. Beyond magnitude 14, this catalog would prepare the arrival of powerful instruments on the Extremely Large Telescopes, which could include radial velocity (RV) follow-up of faint stars and direct imaging of planets around main sequence stars of gigayear ages.

Methods. We used the mass–sma degenerate set of solutions obtained by GaiaPMEX from any value of ruwe to select a sample of bright ($G < 16$) *Gaia* sources whose companions could be in the planetary domain, with a mass of $< 13.5 M_J$. We selected sources whose astrometric signature determined from the ruwe is larger than zero with a significance of $> 2.7\text{-}\sigma$ ($p\text{-value} < 0.00694$).

Results. It led us to identify a sample of 9,698 planet-candidate-hosting sources that have a companion with a mass of possibly $< 13.5 M_J$ and a sma in the range of $\sim 1\text{--}3$ au. We cross-matched our catalog with the NASA Exoplanet Archive (NEA) catalog of exoplanets, identifying 19 of our systems therein. We successfully detected eight confirmed substellar companions with an sma of $1\text{--}3$ au, initially discovered and characterized with RV and astrometry. Moreover, we found six transiting-planet systems and two wide-orbit systems for whom, with GaiaPMEX, we predict the existence of supplementary companions. Focusing on the subsample of sources observed with HIPPARCOS, combining the constraints from ruwe and PMA, we confirm the identification of four new planetary candidate systems, HD 187129, HD 81697, CD-42 883, and HD 105330.

Conclusions. Given the degeneracy of mass–sma, many of the candidates in this catalog of 9,698 sources might have a larger mass in the brown-dwarf and stellar domain if their sma departs from the $1\text{--}3\text{-au}$ range. The vetting of this large catalog will be the subject of future studies.

Key words. exoplanets detection ; astrometry ; radial velocities

1. Introduction

Up to now, the vast majority of exoplanets have been discovered using the transit and radial velocity (RV¹) techniques, as seen for example in the NASA Exoplanet Archive² (NEA) or the *exoplanet.eu* catalog. *Gaia*'s absolute astrometry is expected to reveal (tens of) thousands of new exoplanets and brown dwarfs (BDs) in the near future (Perryman et al. 2014; Sahlmann et al. 2015; Holl et al. 2022; Gaia Collaboration et al. 2023a; Holl et al. 2023). Using the third *Gaia* data release (GDR3; Gaia Collaboration et al. 2021) time series, Holl et al. (2023) recently published 1162 sources with an astrometric-orbit solution, including 9 exoplanet candidates and 29 BD candidates (assuming an M_\star of $1 M_\odot$). Those candidates have masses whose confi-

dence region overlaps with the planetary or BD domain. Based on the Thiele-Innes parameters fitted from the unpublished time series and listed in the *Gaia* DR3 non single star catalog (*Gaia*-NSS), Gaia Collaboration et al. (2023a) reported 1843 BD candidates and 72 exoplanet candidates, among which there are 10 already known BDs, and 9 RV exoplanets validated with *Gaia*'s astrometry, and 2 new exoplanets with masses of 5 and $7 M_J$, which were also identified in Holl et al. (2023).

Given the many thousands of exoplanets expected from *Gaia*, the above-reported number of exoplanet candidates is still below expectations. This could be partly explained by the sparse temporal coverage of orbital phases, which leads to large uncertainties and degeneracies on the orbital solutions. Nevertheless, *Gaia* should allow the detection of numerous Jupiter-mass exoplanets within the range of Earth–Neptune orbits. This range is still underpopulated among the approximately 5000 known exoplanets because of the observation biases inherent to the techniques that yield many of the detections: short-period ($P < 1$ yr) planets are mainly detected and characterised with RV and transits, while high-contrast imaging is most sensitive to super-massive exoplanets and those with a large semi-major axis

[★] Table B.1 is only available in electronic form at the CDS via anonymous ftp to cdsarc.u-strasbg.fr (130.79.128.5) or via <http://cdsweb.u-strasbg.fr/cgi-bin/qcat?J/A+A/>

^{**} Please send any request to flavien.kiefer@obspm.fr

¹ All acronyms used are summarized and indexed in Appendix A.

² <https://science.nasa.gov/exoplanets/exoplanet-catalog/>

($M_p > 5 M_J$; $sma > 5$ au). A key objective is the exploitation of the *Gaia* database in its most recent release (GDR3; Gaia Collaboration et al. 2021) in order to detect unknown exoplanet candidates, such as AF Lep b (Mesa et al. 2023; Franson et al. 2023; De Rosa et al. 2023).

In Kiefer et al. (2024; Paper I hereafter), we introduced a new tool called *Gaia* DR3 proper motion anomaly and astrometric noise excess (GaiaPMEX), which is designed to determine the mass of possible candidate companions and their sma relative to their central star by considering either the astrometric excess noise (AEN; see Kiefer et al. 2019; Kiefer 2019; Kiefer et al. 2021), the renormalized unit weight error (ruwe; see Lindgren et al. 2018, 2021), or the proper motion anomaly (PMA; see Kervella et al. 2019; Brandt 2021; Kervella et al. 2022), or by combining the constraints from the ruwe and the PMA.

In Sect. 2 we briefly describe the theory behind GaiaPMEX and the main properties of the mass– sma solutions found that led us to determine a minimum companion mass compatible with *Gaia*'s astrometry for any source brighter than $G=16$. In Sect. 3 we present a sample of 9,698 sources around which we infer the presence of a companion whose mass could overlap with the planetary domain. This catalog is discussed and compared with other catalogs in Sect. 4.

2. The astrometric minimum mass of companions determined with GaiaPMEX

The GaiaPMEX tool models —within a Bayesian framework— the AEN, ruwe, and PMA as measured by *Gaia* and HIPPARCOS based on the orbital motion of a source's photocenter due to a companion, and accounts for both measurement and instrumental noise. GaiaPMEX provides 2D confidence maps for the mass and sma of a companion based on the individual values of AEN, ruwe, and PMA, and on the constraints from ruwe and PMA combined.

An interesting feature of these confidence maps is that they follow a specific pattern; the maps determined from the AEN and ruwe are V-shaped, while those determined from the PMA are U-shaped. This pattern is well modeled by segmented linear relationships between mass and sma , which are thoroughly detailed in Paper I. These relationships depend on the part of the AEN, ruwe, or PMA in excess of noise, which we call the "astrometric signature". We are particularly interested in the relationships fixed by the value of the ruwe; these are shown in Fig. 1 for the illustrative case of the M-dwarf GJ 832 (see also Paper I for more details).

2.1. The ruwe-based astrometric signature

The ruwe measures the amplitude of residuals relative to the formal errors of the data, once a five-parameter linear model (including centroid position, proper motion, and parallax) has been fitted out of *Gaia*'s astrometric points. From the ruwe, we are able to determine a ruwe-based astrometric signature, referred to here as $\alpha_{\text{UEVA, ruwe}}$. The astrometric signature α_{UEVA} measures the excess in the unbiased estimator of variance a posteriori (UEVA for short) of the five-parameter model residuals, beyond the expectation value of the unbiased estimator of variance a posteriori if the star was actually single:

$$\alpha_{\text{UEVA}} = \sqrt{\text{UEVA} - \text{UEVA}_{\text{single}}}. \quad (1)$$

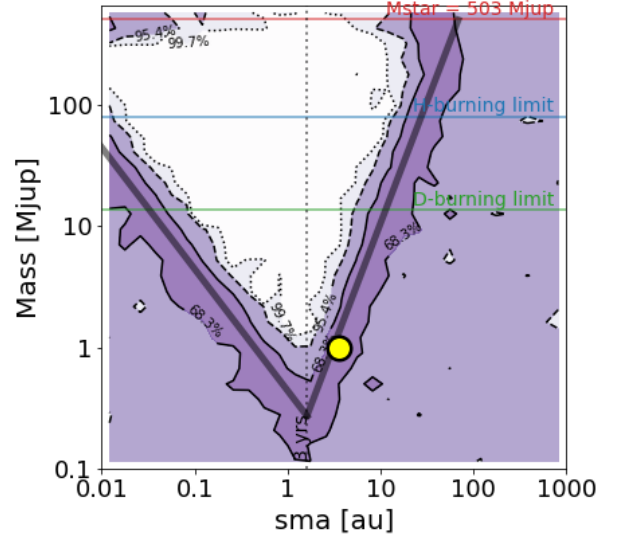


Fig. 1. GaiaPMEX confidence map of the mass and sma of a companion around GJ 832 constrained by the ruwe. The darkest area delineated with a black solid line spans the 68.3% confidence region. The gradually lighter purple areas delineated with black dashed and dotted lines, respectively, span the 95.4% and 99.7% confidence regions. This example is described in detail in Paper I. The thick dark lines show the mass– sma relationship of Eq. 6. The yellow circle shows the $M \sin i$ and sma of the known Jupiter-like planet in this system (Philipot et al. 2023).

The UEVA of a given source can be determined from the value of ruwe^3 using the equation derived in Paper I, that is,

$$\text{UEVA}_{\text{ruwe}} = (\text{ruwe} \times u_0)^2 (\sigma_{\text{att}}^2 + \sigma_{\text{AL}}^2), \quad (2)$$

where u_0 is the factor determined for any source with respect to its G -mag and $Bp - Rp$ in the GDR3 auxiliary data⁴. The σ_{AL} is the error on the astrometric along scan (AL) angle measurements, and σ_{att} is the attitude excess noise, that measures an 'average' calibration noise ~ 0.076 mas among all sources observed at a given epoch.

The single star $\text{UEVA}_{\text{single}}$ is determined from the theoretical approximate normal distribution of the UEVA with respect to typical errors and noise in GDR3 data found in Paper I, $\mathcal{N}(\mu, \sigma)$:

$$\begin{aligned} \mu &= \frac{N_{\text{AL}}}{N_{\text{AL}} N_{\text{FoV}} - 5} \left[(N_{\text{FoV}} - 5) \sigma_{\text{calib}}^2 + N_{\text{FoV}} \sigma_{\text{AL}}^2 \right] \quad (3) \\ \sigma^2 &= \frac{2N_{\text{AL}}}{(N_{\text{AL}} N_{\text{FoV}} - 5)^2} \left[N_{\text{AL}} (N_{\text{FoV}} - 5) \sigma_{\text{calib}}^4 \right. \\ &\quad \left. + N_{\text{FoV}} \sigma_{\text{AL}}^4 + 2N_{\text{FoV}} \sigma_{\text{AL}}^2 \sigma_{\text{calib}}^2 \right], \quad (4) \end{aligned}$$

where σ_{calib} is the calibration noise. The values of σ_{calib} , σ_{AL} and σ_{att} are estimated in Paper I, with respect to the G , $Bp - Rp$, RA, and Dec. of any given sources. N_{FoV} is the number of field of view (FoV) transits detected by *Gaia* (astrometric_matched_transit) and N_{AL} is the average number of astrometric measurement per transit $N_{\text{AL}} = \text{int}(N/N_{\text{FoV}})$, with N the total number of AL angle measurements (astrometric_n_good_obs_al).

³ It could also be determined from the AEN, but as explained in paper I, the ruwe is more reliable for all sources of any $G < 16$.

⁴ <https://www.cosmos.esa.int/web/gaia/auxiliary-data>

2.2. The significance of $\alpha_{\text{UEVA},\text{ruwe}}$

Even if $\alpha_{\text{UEVA},\text{ruwe}}$ is above zero, it remains possible that it only stems from the effect of astrometric noise when observing a single source. In such a case indeed, $\alpha_{\text{UEVA},\text{ruwe}}$ would be said to not be significant. To express the probability for $\alpha_{\text{UEVA},\text{ruwe}}$ to be explained by only noise, we define its significance as the $N - \sigma$ level that corresponds to the one-sided p -value of $\text{UEVA}_{\text{ruwe}}^{1/3}$ in the distribution of $\text{UEVA}_{\text{single}}^{1/3}$. The higher the significance, the lower the probability of a noise-based origin, and thus of singleness. The 1, 2, and 3- σ levels correspond to p -values of respectively 31.7%, 4.6%, and 0.3%. As detailed in paper I, the reason for using the UEVA instead of $\alpha_{\text{UEVA},\text{ruwe}}$ directly, and to the power 1/3, is that (i) α_{UEVA} is undefined whenever $\text{UEVA}_{\text{ruwe}}$ is smaller than $\text{UEVA}_{\text{single}}$, and (ii) according to Wilson & Hilferty (1931) (see also Canal 2005), if X is proportional to a random variable that follows a χ^2 distribution, then $X^{1/3}$ closely follows a normal distribution. This is approximately the case for $\text{UEVA}_{\text{single}}^{1/3}$ (see Sects. 5.2.1 and C in paper I). We therefore assumed that $\text{UEVA}^{1/3}$ followed a normal distribution $\mathcal{N}(\mu_{1/3}, \sigma_{1/3})$ and approximated its parameters by $\mu_{1/3} = \mu^{1/3}$ and $\sigma_{1/3} = \sigma \mu^{-2/3} / 3$ by applying error propagation from Eqs. 3 and 4. It is then straightforward to calculate a p -value for a realisation x using the Python function `scipy.stats.normal.cdf(x, $\mu_{1/3}$, $\sigma_{1/3}$)` and a corresponding $N - \sigma$ using `scipy.stats.normal.ppf(1 - (1 - p)/2)`.

2.3. The mass–sma relationships and the minimum mass

The astrometric signature α_{UEVA} relates the sma and the mass through a formula determined in Paper I, in which the parameters vary with the orbital period of the companion:

$$M_c = C_\ell \frac{\alpha_{\text{UEVA}}}{\varpi} M_\star^{\frac{2-n_\ell}{3}} \text{sma}^{n_\ell}, \quad (5)$$

where the parameters C_ℓ and n_ℓ are fixed to

$$\alpha_{\text{UEVA}} \Rightarrow \begin{cases} \ell=1: <3 \text{ yr}, & n_1 = -1, & C_1 = 2300 \\ \ell=2: >3 \text{ yr}, & n_2 = +2, & C_2 = 260. \end{cases} \quad (6)$$

Those relationships are overplotted on the GaiaPMEX confidence map determined from the ruwe of GJ 832 in Fig. 1. If the $\alpha_{\text{UEVA},\text{ruwe}}$ is significant, which means typically more than 2- σ , these relationships allow us to measure the minimum mass of the companion, located at the minimum of the V-shaped curve. This is reached at an $\text{sma} \sim 2$ au:

$$\alpha_{\text{UEVA},\text{ruwe}} \Rightarrow \begin{cases} M_{c,\text{min}} = 1150 M_\star^{2/3} \times \alpha_{\text{UEVA},\text{ruwe}} / \varpi & (\text{M}_J), \\ \text{sma}_{\text{min}} = 2.1 M_\star^{1/3} & (\text{au}). \end{cases} \quad (7)$$

We use this approximative $M_{c,\text{min}}$ to select a sample of candidate sources that may host a companion down to the planetary domain, whose $M_{c,\text{min}} < 13.5 \text{ M}_J$.

3. A catalog of 9,698 stars with possible exoplanet candidates identified with *Gaia*

3.1. The main steps of the catalog selection

We searched the GDR3 catalog for bright sources with $G < 16$ that show a significant astrometric signature α_{UEVA} compatible

with a companion mass of $< 13.5 \text{ M}_J$. The diagram in Fig. 2 summarizes the various steps of our selection process.

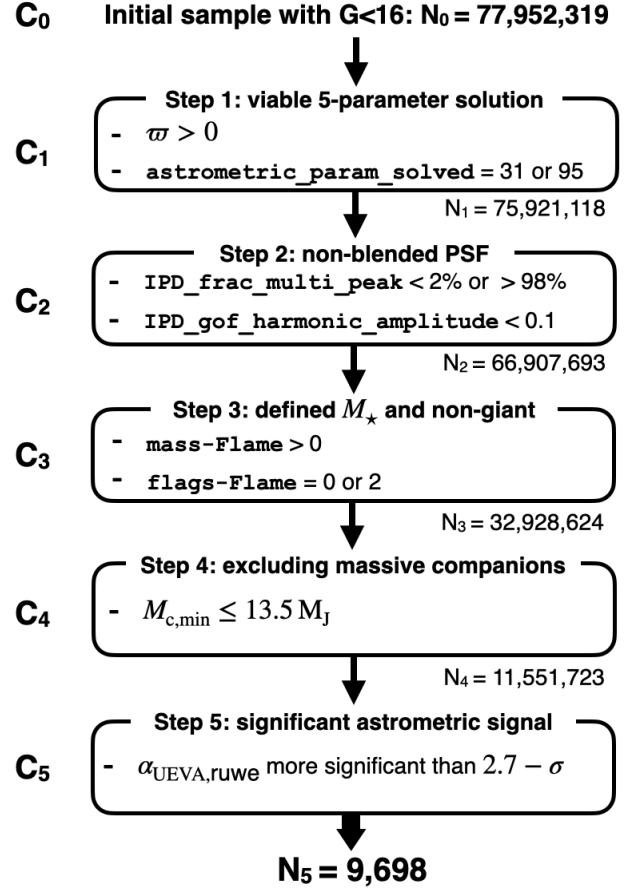


Fig. 2. Selection steps used to build the sample of candidate systems with exoplanet companions, where six selection criteria (C_0 to C_5) are applied iteratively.

As we developed GaiaPMEX specifically for bright sources with $G < 16$ (Paper I), we used here the same parent sample of 77,952,319 sources obtained using this selection criterion, that is $G < 16$. This is our input sample selection criterion C_0 .

In step 1, we selected all sources with a positive parallax⁵ in the 5p and 6p datasets (criterion C_1), which gives a total of 75,921,118 sources, of which 73,582,079 belong to the 5p dataset and 2,339,039 to the 6p dataset. In step 2, applying criterion C_2 , we rejected the sources that show diagnostics of blend in the PSF fitted by the image parameter determination (IPD). As defined in Paper I (see also Fabricius et al. 2021), strong blends in the PSF due to background objects or other multiple components are diagnosed by two IPD indicators published in the GDR3 archive. When `IPD_frac_multi_peak` is typically within 2–98% and `IPD_gof_harmonic_amplitude` > 0.1 , the centroid of the fitted PSF likely underwent strong time-dependent offsets leading to significant residual signals on top of the proper and parallactic motions. Removing the sources satisfying these criteria led to the selection of 66,907,693 sources (65,677,199 in the 5p dataset and 1,230,494 in the 6p dataset).

In step 3, we applied our third selection criterion (C_3). We identified the sources with a well-defined and nongiant stellar mass in the GDR3 Coordination unit 8 database (CU8; Gaia

⁵ Few sources have an ill-defined negative or null parallax. Those are discarded.

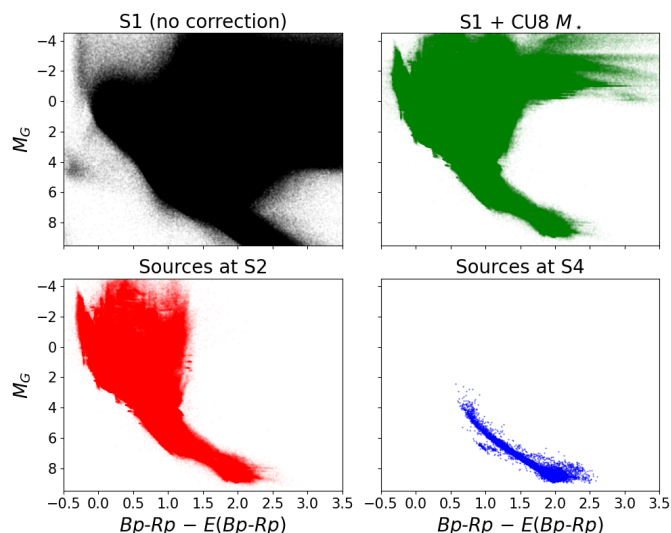


Fig. 3. Hertzsprung-Russell diagrams throughout the sequence of the selection steps presented in Fig. 2. The different steps are shown as follows: the sources at S1 whose absolute magnitude M_G is not corrected for extinction and $Bp - Rp$ is not corrected for reddening are shown in black; the sources with an existing mass in the CU8 catalog and whose G and $Bp - Rp$ are corrected for extinction and reddening are shown in green, and those that are moreover nongiant and without photometric mass are shown in red; and the final 9,698 planet-candidate hosts are shown in blue.

Collaboration et al. 2023b). Only about 140 million of the 1.6 billion stars in the full GDR3 catalog have a proposed stellar mass of within $0.5\text{--}10 M_\odot$ as determined by combining photometry, parallax, and stellar models, the so-called mass-Flame in the CU8 database, which is also written $M_{\star, \text{Flame}}$. A flag called flags-Flame, a two-characters string AB where A and B are either "0", "1", or "2", indicates the quality of the mass estimation in CU8 (see details in Gaia Collaboration et al. 2023b). We excluded stars identified as giants (A=1 in +flags-Flame+), and those for which the distance was estimated photometrically (by GSP-phot; B=1 in +flags-Flame+) and is thus possibly inaccurate given the binarity of the stars that we are considering. This led us to select 32,928,624 sources, among which 32,422,316 and 506,308 are in the 5p and 6p datasets, respectively. Figure 3 shows the Hertzsprung-Russell diagram of all these sources and how they are reduced when: selecting sources given a defined CU8 $M_{\star, \text{Flame}}$, and then excluding giants and masses determined using photometric distances. In this diagram, we use the absolute magnitude and $Bp - Rp$ color corrected for extinction and reddening for the sources whose mass was found in the CU8 catalog; otherwise the absolute magnitude was obtained as $M_G = G - 5 \log \varpi + 10$. Those sources not found in the CU8 catalog are of diverse types, including evolved states—giants and white dwarfs—whose masses are more difficult to estimate.

In step 4, using our knowledge of $M_{\star, \text{Flame}}$, ruwe, and parallax (ϖ), as well as the noises derived from the G -mag, $Bp - Rp$, RA, and Dec., we determined the mass by minimizing the GaiaPMEX curves for ruwe and $M_{c, \text{min}}$ using Eq. 7. As we are interested in the planet candidates, we selected only those with $M_{c, \text{min}} < 13.5 M_J$ (criterion C_4). This led us to select a total of 11,551,723 systems, among which 11,342,194 are in the 5p dataset, and 209,529 in the 6p dataset.

Finally, in step 5, we selected the sources for which, additionally, we have strong evidence of astrometric motion (criterion C_5). We selected the sources whose significance of α_{UEVA} is

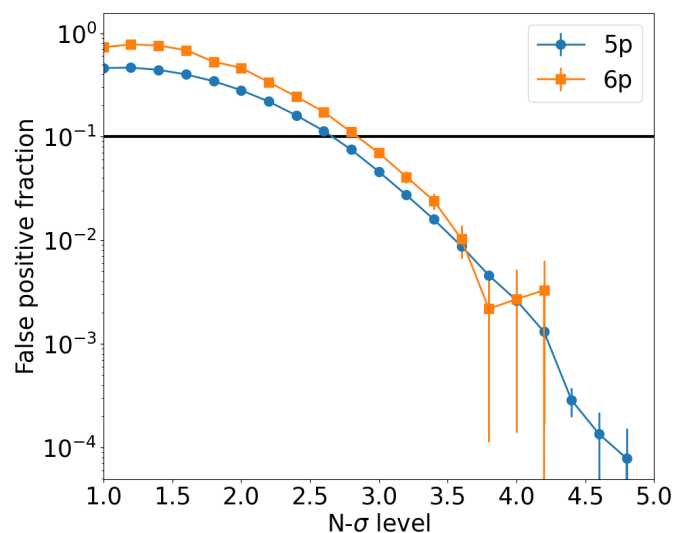


Fig. 4. Fraction of FPs among selected planet candidates at different significance criteria ($N\text{-}\sigma$) in the 5p (blue) and 6p (orange) datasets. The black solid line shows the 10% level.

greater than some threshold, $X\text{-}\sigma$, which optimizes the number of single-star false positives (FPs) among the selected planet-candidate hosts sample. Those FPs would be single stars whose noise mimics the astrometric signature of stars with companions. The definition of α_{UEVA} and its significance are described in Sects. 2.1 and 2.2. As we are interested in gathering as many candidates as possible, whilst keeping the number of FP single stars to 10% of the selected sample at most, we optimized the adopted significance threshold. The FP fraction at any $X\text{-}\sigma$ threshold is the number of FPs divided by the number of α_{UEVA} that are more significant than $X\text{-}\sigma$ and lead to a companion mass of $< 13.5 M_J$. We estimated this fraction using the following methodology. We took the sample defined in step 3 with $N_{S3} = 32,928,624$ sources, and simulated—for all of these sources—values of UEVA and α_{UEVA} as if they were all single stars, that is, only considering stochastic astrometric variability. To do so, we drew values of $\text{UEVA}^{1/3}$ from the normal distribution $\mathcal{N}(\mu_{1/3}, \sigma_{1/3})$ defined in Sect. 2.1 (Eqs. 3 and 4), from which we derived UEVA and α_{UEVA} . Using Eq. 7, we calculated the corresponding minimum masses, and selected those of $< 13.5 M_J$ (criterion C_4). Then, we selected the sources with $\text{UEVA}^{1/3}$ more significant than $X\text{-}\sigma$ (criterion C_5). This led to a FP planet sample at X with a size of $N_{\text{FP},0}$. However, since a large fraction of the 32,928,624 sources are truly multiple, and thus not single, $N_{\text{FP},0}$ overestimates the actual number of FP. A more realistic size of the single-star population in the input sample is obtained by (i) removing the sources with $\text{UEVA}_{\text{ruwe}}^{1/3}$ larger than $X\text{-}\sigma$, and (ii) dividing the size, $N_{X\text{-}\sigma}$, of this residual sample by the theoretical proportion, $r_{X\text{-}\sigma}$, below $X\text{-}\sigma$ significance. For instance, $r_{X\text{-}\sigma}$ takes values of 0.683, 0.954, or 0.9973 if $X=1, 2$, or 3 , respectively. This leads to $N_{\text{FP}} = N_{\text{FP},0} \times (N_{X\text{-}\sigma} / r_{X\text{-}\sigma}) / N_{S3}$, of which the FP fraction among candidate-planet systems beyond $X\text{-}\sigma$ significance can be determined. We tested many values of $X\text{-}\sigma$ significance from 1 to 5, and reproduced the whole process ten times to determine the mean and standard deviation of the FP fraction as a function of the significance level. This is shown in Fig. 4. The FP fraction is smaller than 10% when selecting planet candidates whose $\alpha_{\text{UEVA}, \text{ruwe}}$ is at least above the $2.7\text{-}\sigma$ significance level, that is, with $p\text{-value} < 0.006934$. Adopting this $2.7\text{-}\sigma$ level led us to select a sample of 9,698 sources, among which 9,587 sources

are in the 5p dataset, and 111 are in the 6p dataset. Being more selective on criterion C_5 leads to subsamples of 6,552 systems adopting a $3\text{-}\sigma$ significance level ($p\text{-value}<0.0027$), and 2,268 with $4\text{-}\sigma$ ($p\text{-value}<0.000063$). Those datasets would have a FP fraction of about 6% and 0.2%, respectively. The full catalog of the 9,698 candidate sources is available at the CDS, with a small extract shown in Table B.1. We ordered the catalog in increasing magnitude in G -band. The source with ID # 1 has the smallest magnitude, of 5.99, and the source with ID # 9698 has the highest magnitude, of 15.53.

3.2. Sample description

The Hertzsprung-Russell diagram of the planet-candidate hosts sample is shown in Fig. 3. While at step 3 some subgiants remain in the sample, all selected planet-candidate hosts at step 5 (in blue) are located along the main sequence. This is explained by the selection of sources with $M_{\star,\text{Flame}}$ of mostly $<1 M_{\odot}$.

Figure 5 shows the distribution of planet-candidate hosts across the sky. They are homogeneously distributed compared to the full input sample at step 3. The hosts are thus field stars that are relatively close to the Sun.

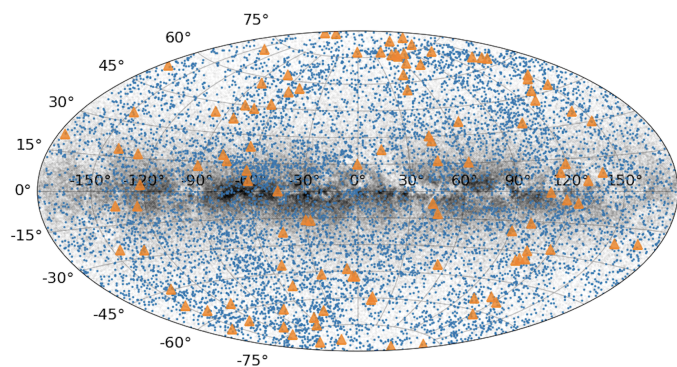


Fig. 5. Distribution of the locations in the plane of the sky, in galactic coordinates, of planet-candidate hosts from the 5p (blue) and 6p (orange) datasets, compared to all the sources in the input sample at step 3 (black).

Figure 6 represents the number of planet-candidate hosts with respect to ϖ and M_{\star} . It can be seen that all planet candidate hosts are indeed close-by with $\varpi>2.9$ mas ($d<345$ pc), and that most planet candidates are found around stars with $M_{\star}<0.8 M_{\odot}$ and $\varpi<20$ mas; that is, M and K-dwarfs beyond 50 pc. This is the result of both the increase in the volume of stars with increasing distance and the increase in the detectability of planets around fainter stars with smaller M_{\star} and larger ϖ . This is also clear when comparing the distribution of planet-candidate hosts to the distribution of sources in the input sample at step 3 (shown as white contours), and the modulation of the sensitivity of *Gaia*'s ruwe for the detection of 2–13.5 M_{J} companions within 1–3 au (shown as red contours) with respect to M_{\star} and ϖ . The sensitivity levels are obtained as explained in Sect. 9 of Paper I. On a grid of 30×30 bins of M_{\star} and ϖ , we simulated—for each bin—1000 values of UEVA for our reference system GJ 832 assuming a companion with a mass of within 2–13.5 M_{J} and an sma of within 1–3 au. The sensitivity, at any M_{\star} and ϖ , is the percentage of simulations with an UEVA more significant than $2.7\text{-}\sigma$.

Figure 7 shows the distribution of the minimum mass of the planet candidates with respect to the G -mag and M_{\star} of the hosts. Planet candidates with $M_{c,\text{min}}<5 M_{\text{J}}$ are mostly detected around sources with $G\sim 14$. Those correspond to low-mass stars, namely

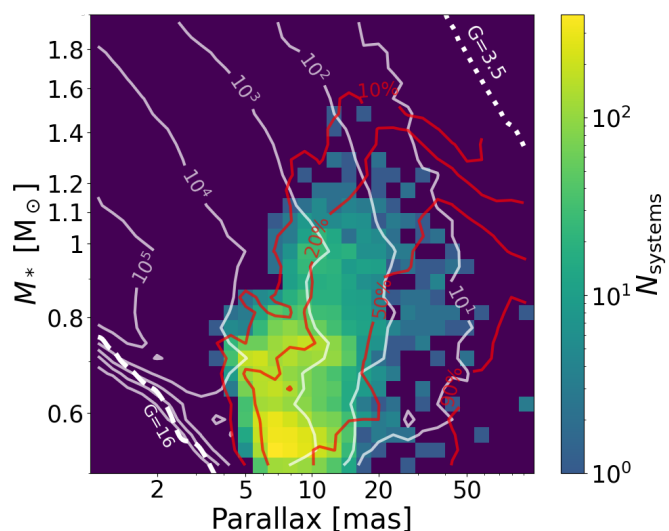


Fig. 6. Number of detected planet candidates (per bin) with respect to parallax and M_{\star} . The sensitivity curve of *Gaia* for detecting 2–13.5 M_{J} companions at 1–3 au beyond a significance of $2.7\text{-}\sigma$ is overplotted in red showing the regions where more than 10, 20, 50 and 90% of companions are detected. The distribution of the *Gaia* sources satisfying steps 1–3 (Fig. 2) is also overplotted in white solid lines. The dashed thick white lines bound the region within the magnitude range of our sample, that is G -mag within 3.5–16.

MK-dwarfs with $M_{\star}<0.7 M_{\odot}$. We did not include M-dwarfs with masses of $<0.5 M_{\odot}$ because we used the mass-Flame of the CU8 catalog, which is only determined for stars with masses of $>0.5 M_{\odot}$. This explains why we do not detect planet candidates with $M_{c,\text{min}}<5 M_{\text{J}}$ beyond $G=14$. Nonetheless, M-dwarfs offer the best opportunity to detect exoplanets with *Gaia*.

The candidate exoplanets are compared to the known exoplanet population taken from the NASA Exoplanet Catalog⁶ in the mass–sma diagram presented in Fig. 8. Because of the geometry of the V-shaped curve, whose minimum lies at about 2 au, the sma of the exoplanet candidates are all contained at most within 0.1–10 au. Extrapolating along the empirical mass–sma relationships presented in Sect. 2, we delineated the wider region of possible mass and sma spanned by the exoplanet candidates with $\text{sma}\neq 2$ au. This exercise shows that the current domain of sensitivity of *Gaia* allows us to probe exoplanets that can be further confirmed and characterized using RVs. Moreover, the set of solutions covers a domain of orbits for Jupiter-like exoplanets that are less represented between 0.1 and 1 au, which is on the border of the orbit circularization zone (Kane 2013). The full set of solutions extend to within the BD desert below orbital periods of 80 days (Kiefer et al. 2019, 2021), that is $\text{sma}<0.36$ au for a $1M_{\odot}$ host star. If some of the candidates are found to not be exoplanets and with an $\text{sma}<0.4$ au, then they may become newly identified BD.

4. Discussion

The complete vetting of our catalog of 9,698 planet-candidate hosts will be the subject of future studies. Nevertheless, we searched the *Gaia*-NSS (Gaia Collaboration et al. 2023a), and found 339 sources with an orbital solution among our 9,698 planet-candidate hosts. Moreover, we searched the Centre de Données de Strasbourg (CDS) and found 2,951 sources refer-

⁶ <https://exoplanetarchive.ipac.caltech.edu>

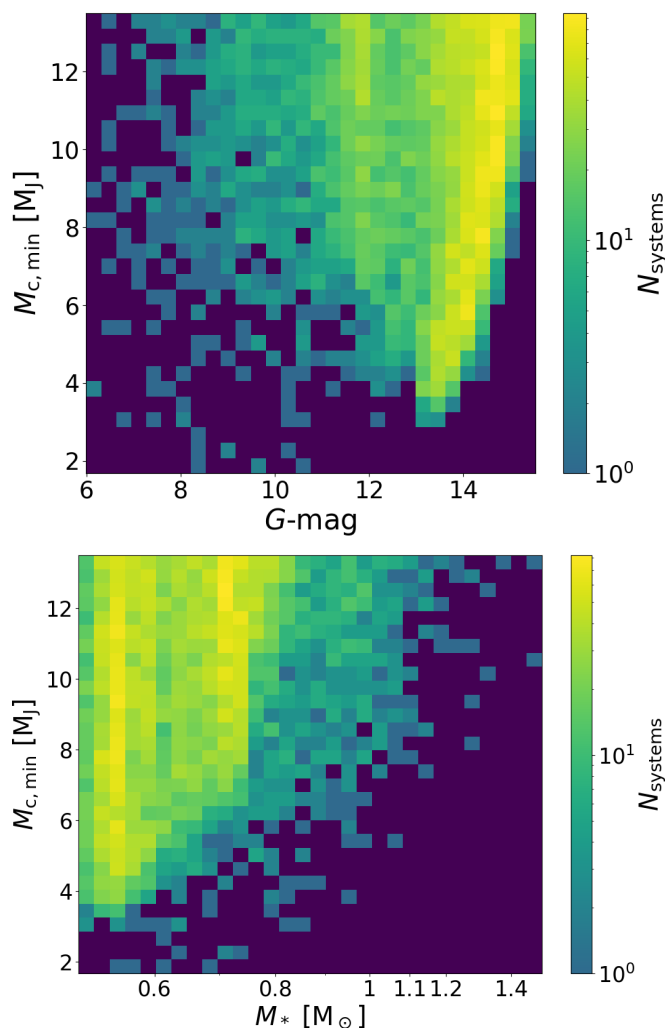


Fig. 7. Number of detected planet-candidate hosts (per bin) with respect to the minimum mass of the companion and the G -magnitude or mass of the host star (top and bottom, respectively).

enced in Simbad, including 286 that were published in the Washington Double Star catalog (WDS; Mason et al. 2001). These latter sources are listed in Table B.1, where the *Gaia*-NSS sources are flagged and the WDS names are given when known. In Sect. 4.1 we describe the ruwe-based astrometric signatures and the astrometric orbital solutions of the validated *Gaia*-NSS orbits presented in Holl et al. (2023), and cross-check our catalog of planet candidate hosts with their estimation of the companion mass. In Sect. 4.2 we cross-match our catalog with the exoplanets listed in the NEA. Finally, in Sect. 4.3 we focus on those of our selected systems that were observed with HIPPARCOS and for which the PMA can help in characterizing the sma and mass of the identified companion.

4.1. A comparison with *Gaia*-NSS-validated orbits and planet-candidate cross-match

Holl et al. (2023; H23) identified and validated the astrometric orbits for 204 sources published in the *Gaia*-NSS catalog with an orbital period of <5.6 yr, and further characterized in *Gaia* Collaboration et al. (2023a). We compared the ruwe-based astrometric signatures determined in this work to those deduced from the astrometric orbits, and cross-checked our planet selec-

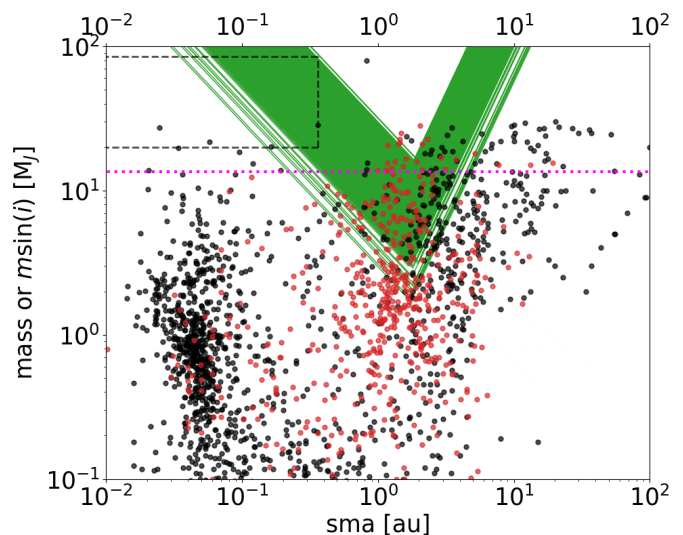


Fig. 8. Mass–sma diagram of known exoplanets and planet candidates presented in the current work. The green lines show the degenerate mass and sma compatible with the GDR3 α_{UEVA} . The data for exoplanets are taken from the NEA, including those with a known mass (black dots) and those with only a minimum mass $m \sin i$ (red dots). The black dashed lines bound the BD desert region extending up to orbital periods of 80 days (~ 0.36 au for a $1 M_{\odot}$ host star; Kiefer et al. 2019, 2021). The magenta dotted line represents the commonly accepted $13.5 M_{\text{J}}$ upper-mass limit on the planetary domain.

tion with the classification of H23 according to the estimated companion mass.

4.1.1. Comparing the $\alpha_{\text{UEVA,ruwe}}$ and the orbital solutions

Among the 204 sources of H23, two have a G -mag of >16 and hence are not part of our present sample, namely DENIS J082303.1-491201 and 2MASS J08053189+4812330, two BDs with respective G -mag of 18.5 and 20. The other 202 sources have $G < 16$, and are listed in Table D.1. Among them, 196 are well behaved, verifying criteria $C_0 \cap C_1$, as defined in Fig. 2, 101 of which have a mass-Flame characterized in the CU8 database and are located on the main sequence (criteria $C_0 \cap C_1 \cap C_2$). We find that $\sim 93\%$ of the H23 sample, that is 184 of the 196 well-behaved sources, including 93 of the 101 with a mass-Flame, have an $\alpha_{\text{UEVA,ruwe}}$ that is more significant than $2.7\text{-}\sigma$ (criteria $C_0 \cap C_1 \cap C_4$). Only 12 sources are found to meet all the selection criteria of our planet-candidate hosts sample.

H23 classified the companions of their 204 sources into three categories with respect to their mass range if their host star had a mass of $1 M_{\odot}$: pseudo-mass-index=0 if $<20 M_{\text{J}}$ (11 sources), pseudo-mass-index=1 if within $20\text{-}120 M_{\text{J}}$ (32 sources), and pseudo-mass-index=2 if $>120 M_{\text{J}}$ (161 sources). At a pseudo-mass-index of 0, of the 10 well-behaved sources, 5 have an $\alpha_{\text{UEVA,ruwe}}$ more significant than $2.7\text{-}\sigma$. At a pseudo-mass-index of 1, that is 29 among 31 well-behaved sources. At a pseudo-mass-index of 3, that is 150 among 156 well-behaved sources. Thus, in 94-96% of the cases, companions in the BD and stellar mass regime that are detected and characterized with the *Gaia* astrometric time series are associated with an $\alpha_{\text{UEVA,ruwe}}$ more significant than $2.7\text{-}\sigma$. In the planetary regime, at a pseudo-mass index of 0, this rate is $\sim 50\%$. This means that, unsurprisingly, due to the necessity of defining a threshold on the significance of $\alpha_{\text{UEVA,ruwe}}$, a large fraction of planetary companions were missed.

Within the H23 sample, we find 11 sources with an $\alpha_{\text{UEVA},\text{ruwe}}$ that cannot reject the single-star hypothesis, at a p -value of smaller than the $2.7\text{-}\sigma$ threshold. More specifically, we identify:

- AK For, HD 106770, HD 188622, and HD 211419, which have an $\alpha_{\text{UEVA},\text{ruwe}}$ significance of within $2\text{--}2.7\text{-}\sigma$; whether they can be considered as detected or not is disputable, because the $2\text{-}\sigma$ threshold could also have been adopted, more conventionally, so as to reject the null hypothesis with a p -value of $<4.6\%$. We recall that, for the sake of keeping an FP rate below 10%, we had to adopt a more restrictive threshold of $2.7\text{-}\sigma$;
- HD 142, ι Hor, TYC 8841-182-1, HIP 66074 (*Gaia*-3), HD 184962, HD 100069, and HD 132406, each with a significance smaller than $2\text{-}\sigma$;
- HD 142 and AK For, for which the PMA rejects the single-star hypothesis with a significance of respectively $2.8\text{-}\sigma$ and more than $9\text{-}\sigma$: GaiaPMEX thus detects the known companion in both cases.

The scale of the α_{UEVA} expected from the mass and period of their companions and the parallax can explain this lower significance. Figure 10 compares the $\alpha_{\text{UEVA},\text{ruwe}}$ to the $\alpha_{\text{UEVA},\text{H23}}$ calculated from the known *Gaia* astrometric solutions of the H23 list in Gaia Collaboration et al. (2023a) and the empirical relations in Eq. 6, as explained in Appendix C. The $\alpha_{\text{UEVA},\text{ruwe}}$ and the $\alpha_{\text{UEVA},\text{H23}}$ generally agree to within an order of magnitude in the range 0.1–10 mas. Therefore, our estimation of the astrometric signatures from the RUWE is generally compatible with the mass and sma of companions around sources with fitted astrometric orbits.

Apparent counter-examples to this statement are HD 134251, HD 108510, HD 221757, HD 117126, and HD 8054, which all lead to overestimation of $\alpha_{\text{UEVA},\text{H23}}$ compared to $\alpha_{\text{UEVA},\text{ruwe}}$ by a factor of >2.5 and even >3 (HD 134251 and HD 108510). These are all binaries (pseudo-mass index of 2). We find no satisfactory explanation for this discrepancy, while RV-SB1 solutions tend to validate the orbital parameter and mass of the companion used to calculate $\alpha_{\text{UEVA},\text{H23}}$.

In that regard, the case of HIP 66074, which has $\alpha_{\text{UEVA},\text{H23}}/\alpha_{\text{UEVA},\text{ruwe}}=2.4$, is interesting, as its companion is *Gaia*-3 b, a planet (Winn 2022; Marcussen & Albrecht 2023). Here, the mismatch might be related to an issue with the astrometric solution published in the *Gaia*-NSS, which is inconsistent with the RV solutions for this system. Both predict an edge-on inclination, but do not agree on the mass of the companion *Gaia*-3 b, suggesting $7.3 M_{\text{J}}$ (*Gaia*-NSS) and $0.4 M_{\text{J}}$ (RV). From the *Gaia*-NSS solution, we predict $\alpha_{\text{UEVA},\text{H23}}=0.093\pm 0.014$ mas, while we find a $1.1\text{-}\sigma$ significant $\alpha_{\text{UEVA},\text{ruwe}}=0.041$ mas. Such a small insignificant α_{UEVA} would rather be compatible with the small-mass estimated by RV. This is in tension with the results from Sozzetti et al. (2023), who propose, to reconcile the RV and *Gaia*-NSS solutions, a companion with a mass of $3\text{--}7 M_{\text{J}}$ on a face-on orbit. This solution would still imply a much larger value of α_{UEVA} of close to 0.1 mas, with a significance certainly beyond $2.7\text{-}\sigma$. Nevertheless, Sozzetti et al. (2023) proposed that the sma of the photocenter in the *Gaia*-NSS solution could be overestimated by up to a factor ~ 2 . In such a case, the astrometric signatures would indeed better match, with now $\alpha_{\text{UEVA},\text{H23}}=0.047\pm 0.007$ mas. According to Sozzetti et al. (2023), this would suggest an inclination of $\sim 13^\circ$ for this planet, and a mass of $\sim 3 M_{\text{J}}$. Figure 9 shows the GaiaPMEX map obtained for HIP 66074, combining ruwe and PMA and comparing these to the possible masses of the companion *Gaia*-3 b.

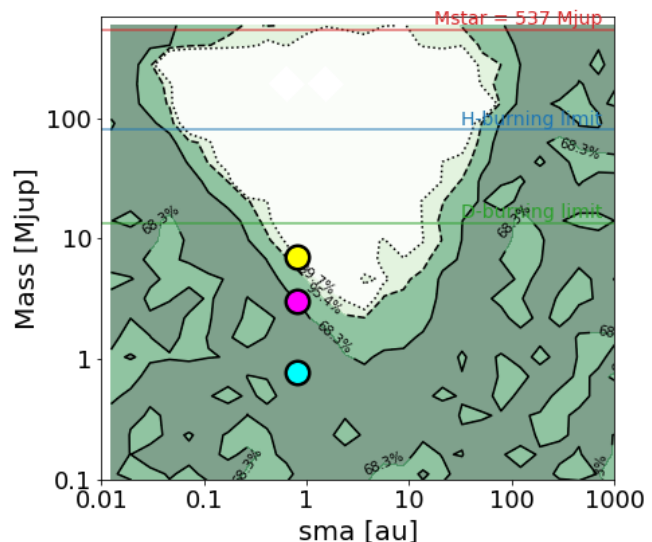


Fig. 9. Same as Fig. 12 but for HIP 66074. Individual maps based on either PMA or ruwe only are shown in Fig. E.2. The yellow and cyan points show respectively the 7 and $0.79 M_{\text{J}}$ solutions at 0.8 au from the *Gaia*-NSS and the RV. The magenta point shows the solution at $3 M_{\text{J}}$ if the photocentric sma measured in the *Gaia*-NSS is overestimated by a factor 2, corresponding to an inclination of 13° .

4.1.2. A cross-match of our planet catalog with the H23 classification

We cross-matched the H23 sample with our catalog of planet-candidate hosts. Among the eight sources at a pseudo-mass index of zero and meeting the criteria $C_0 \cap C_1 \cap C_2$, we find five that belong to our catalog. Moreover, we find that 7 of the 93 sources with a pseudo-mass index 1 or 2 also belong to our catalog. As expected, because of the mass–sma degeneracy, our selection process indeed picks up systems with companions that have a mass above the planetary regime. The five sources listed in our catalog at a pseudo-mass index of zero are HD 40503 (with ID # 212), HD 164604 (# 302), HD 111232 (# 42), HD 81040 (# 56), and HD 175167 (# 74). Four companions, HD 164604 b, HD 111232 b, HD 81040 b and HD 175167 b, are already known exoplanets and are discussed in Sects. 4.2 and 4.3.

The criteria C_4 and C_5 applied on the H23 input sample of 101 systems with a characterized CU8 mass–Flame led to the selection of 12 systems, that is 12% of this input sample. Among the BD/star companions, criteria C_4 and C_5 led to the selection of 7.5% of them, and among the planets, the same criteria led to the selection of 62.5% of them. This implies that our criteria for selecting systems with a possible planetary mass companion within a sample of systems whose M_\star is known are about eight times more likely to select planets than to select BD or stellar companions in the range of orbits where *Gaia* is sensitive. This shows that the significance of α_{UEVA} is a valid criterion for identifying companions whose orbits can be validated afterward, either using astrometric time series published with the fourth *Gaia* data release (GDR4) or other means such as RV or direct imaging.

We conclude that, even though we have identified a few apparent inconsistencies between the observed astrometric signature and the orbital fit of the astrometric time series, they generally agree. We can thus expect that the orbital astrometric motion of most of the planet-candidate-host stars identified in Sect. 3 that have $\alpha_{\text{UEVA},\text{ruwe}} > 0.1$ mas and a period of < 10 yr could be

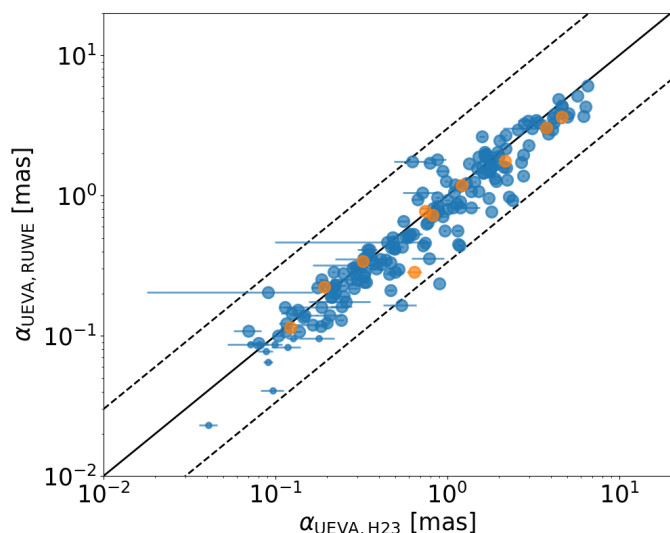


Fig. 10. Comparing the $\alpha_{\text{UEVA}, \text{ruwe}}$ determined in the GDR3 to those calculated from the known astrometric parameters of a companion in Holl et al. (2023) and Gaia Collaboration et al. (2023a). The blue and orange circles show the sources from respectively the 5p and 6p datasets. Tiny-sized symbols indicate a significance of $\alpha_{\text{UEVA}, \text{ruwe}} < 2.7\text{-}\sigma$. The solid line shows the equality, and the dashed lines depict factors of 3 differences, between the data of the two axis.

characterized with the publication of the astrometric time series with the GDR4.

4.2. A cross-match with planet and binary catalogs

Among the 5,678 planets from 4,236 planetary systems published in the NEA, we find 3,793 sources to be brighter than $G=16$ in the 5p and 6p datasets of the GDR3 catalog. Only 2,423 have a mass-Flame, and among those, 149 have an $\alpha_{\text{UEVA}, \text{ruwe}}$ more significant than $2.7\text{-}\sigma$. Finally, 19 systems have an astrometric minimum mass of below $13.5 M_{\text{J}}$ and belong to our sample of planet-candidate hosts, all of them in the 5p dataset. We note that therefore 130 NEA planetary systems must host a BD or stellar companion, instead or on top of the existing planetary companion(s) in those 130 systems. The detailed study of this binary subsample will be within the scope of a future study. We list the 19 planetary systems present in our 9,698 sample in Table B.1, and give details on each below. We determined the GaiaPMEX maps from the ruwe in Fig. F.1. For the sources that were also observed by HIPPARCOS, the constraints from PMA could also be used in combination with the ruwe.

2MASS J04372171+2651014 (# 6883). This low-mass pre-main sequence 2.5 ± 0.4 -Myr-old M-dwarf located at 128 pc is known to host a $4 M_{\text{J}}$ companion, 2M0437 b, at $\sim 118 \pm 1.3$ au (Gaidos et al. 2022). The ruwe=1.21 for this 14.3 mag star corresponds to an $\alpha_{\text{UEVA}, \text{ruwe}} = 0.096$ mas with a $3.3\text{-}\sigma$ significance. The GaiaPMEX map for this star seems to report the detection of a companion at less than 100 pc. However, we would tend to be rather cautious in this case as, for a star as young as 2M0437, one may expect significant accretion, which could induce an astrometric jitter if $L_{\text{acc}}/L_{\star} > 10^{-3}$. We also noted in the epoch photometry available from the online single-object search engine of the Gaia archives that two photometric points in the *B* and *R* bands (on 18 Oct 2015 and 5 Aug 2016) were anomalous. This may indicate possible issues

with the corresponding astrometric points too.

HD 111232 (# 42). This G8V star located at 29 pc is known to host two RV companions (Mayor et al. 2004), including one planet, HD 111232 b, of $7.965^{+1.128}_{-0.479} M_{\text{J}}$ at $2.148^{+0.088}_{-0.097}$ au, and one brown dwarf, of $18.1^{+4.2}_{-1.6} M_{\text{J}}$ at $17.25^{+2.158}_{-2.151}$ au (Feng et al. 2022). Our GaiaPMEX map for HD 111232, combining the constraints from ruwe (1.24; $3.6\text{-}\sigma$) and PMA ($0.54 \pm 0.03 \text{ mas yr}^{-1}$; $>9\text{-}\sigma$), predicts a $4\text{--}50 M_{\text{J}}$ companion within $2\text{--}10$ au of the star with 95.4% confidence. This prediction is in nice agreement with the published parameters of HD 111232 b.

HD 136118 (# 16). This F9V star located at 52 pc is known to host one RV companion of $M \sin i \sim 11.9 M_{\text{J}}$ and $\text{sma} \sim 2.3$ au (Fischer et al. 2002). Using the Hubble Fine Guidance Sensor, Martioli et al. (2010) further showed that this planet candidate is a true BD with a mass of $42^{+11}_{-8} M_{\text{J}}$ at 2.36 ± 0.05 au. Our GaiaPMEX map for HD 136118, combining the constraints from ruwe (1.43; $3.3\text{-}\sigma$) and PMA ($0.43 \pm 0.03 \text{ mas yr}^{-1}$; $5.1\text{-}\sigma$), predicts a $>8 M_{\text{J}}$ companion with an $\text{sma} < 10$ au with 95.4% confidence. It moreover predicts a mass of within $8\text{--}40 M_{\text{J}}$ if the $\text{sma} \sim 2.4$ au. This is in better agreement with the published parameters for HD 136118 b within error bars than the findings of Feng et al. (2022), who predicted a mass within $13.10^{+1.35}_{-1.27} M_{\text{J}}$.

HD 13808 (# 89). This K2V star located at 29 pc is known to host two RV planets (Mayor et al. 2011; Ahrer et al. 2021) with minimum masses of $0.03599 \pm 0.0025 M_{\text{J}}$ at 0.11 au, and $0.0315 \pm 0.0038 M_{\text{J}}$ at 0.26 au. Our GaiaPMEX map for HD 13808, combining the constraints from ruwe (1.17; $2.9\text{-}\sigma$) and PMA ($0.037 \pm 0.026 \text{ mas yr}^{-1}$; $0.4\text{-}\sigma$), predicts a $>2 M_{\text{J}}$ companion within 2 au of the star with 95.4% confidence. It moreover predicts a mass rather in the BD domain in this $2\text{-}\sigma$ confidence region, for at least one of the two planet candidates. This would imply an almost face-on system with an inclination of $< 0.3^\circ$. With an insignificant PMA, this result is mainly driven by the ruwe, which corresponds to $\alpha_{\text{UEVA}, \text{ruwe}} = 0.12$ mas.

HD 164604 (# 302). This K3.5V star located at 39 pc is known to host one RV planet (Arriagada et al. 2010), with $M \sin i = 2.7 \pm 1.3 M_{\text{J}}$ at 1.3 ± 0.5 au. The orbit directly fitted to the astrometric points in the GDR3 (Gaia Collaboration et al. 2023a) led to a larger mass of $14 \pm 5.5 M_{\text{J}}$. Our GaiaPMEX map for HD 164604, combining the constraints from ruwe (1.16; $6.3\text{-}\sigma$) and PMA ($0.55 \pm 0.08 \text{ mas yr}^{-1}$; $6.2\text{-}\sigma$), predicts a $>5 M_{\text{J}}$ companion with an $\text{sma} < 10$ au with 95.4% confidence. At 1.3 au, GaiaPMEX predicts a mass of within $10\text{--}30 M_{\text{J}}$, in agreement with the results of Gaia Collaboration et al. (2023a).

HD 175167 (# 74). This G5IV/V star located at 71 pc is known to host one RV planet (Arriagada et al. 2010), with $M \sin i = 7.8 \pm 3.5 M_{\text{J}}$ at 2.4 ± 0.05 au. The orbit directly fitted to the astrometric points in the GDR3 (Gaia Collaboration et al. 2023a; Winn 2022) led to a larger mass of $14.8 \pm 1.8 M_{\text{J}}$. Later combination with MIKE+FPS by Gan (2023) led to a slightly lower mass of $10.2 \pm 0.4 M_{\text{J}}$. Our GaiaPMEX map for HD 175167 combining the constraints from ruwe (1.17; $3.1\text{-}\sigma$) and PMA ($0.19 \pm 0.02 \text{ mas yr}^{-1}$; $4.1\text{-}\sigma$) predicts a $>5 M_{\text{J}}$ companion with an sma mostly < 10 au with 95.4% confidence. At 2.4 au, GaiaPMEX predicts a mass within $6\text{--}20 M_{\text{J}}$ with 95.4% confidence and $7\text{--}15 M_{\text{J}}$ with 68.3% confidence. This agrees well with the results from Gan (2023).

HD 221287 (# 64). This F7V star located at 53 pc is known to host one RV companion of $M \sin i = 3.1 \pm 0.8 M_{\text{J}}$ and

$sma=1.25\pm 0.4$ au (Naef et al. 2007). To our knowledge, this RV planet has never been confirmed. Our GaiaPMEX map for HD 136118, combining the constraints from ruwe (1.2; $3-\sigma$) and PMA (0.026 ± 0.027 mas yr $^{-1}$; $0.34-\sigma$), predicts a $>3-M_J$ companion with an sma of <3 au with 95.4% confidence. It moreover predicts a mass of within 3–40 M_J if the sma is ~ 1.3 au at 95.4% confidence and within 10–20 M_J at 68.3% confidence. This agrees with the published RV-derived parameters for HD 221287 b but does not confirm the planetary nature of this object.

HD 23596 (# 29). As already discussed in Paper I, for this 7.2-mag F8 star at 52 pc, the combination of PMA (0.59 ± 0.04 mas yr $^{-1}$; $7.1-\sigma$) and ruwe (1.35; $3.5-\sigma$) led GaiaPMEX to infer a companion in the BD domain, with a narrow constraint on mass of 10–30 M_J , as well as on sma, namely 2–5 au at 68.3% confidence. This is in perfect agreement with the known companion of HD 23596 at 2.90 ± 0.08 au, first discovered as an 8.2 M_J super-Jupiter with the ELODIE spectrograph (Perrier et al. 2003), and further re-established as a 14 M_J low-mass BD combining RVs and HIPPARCOS–*Gaia* PMA (Feng et al. 2022; Xiao et al. 2023).

HD 28254 (# 51). This G1IV/V star located at 56 pc is known to host one RV planet (Naef et al. 2010), with $M \sin i=1.16^{+0.1}_{-0.06}$ M_J at 2.15 ± 0.05 au. Combining RV with HIPPARCOS–*Gaia* astrometry led to a larger mass of 1.5–6.5 M_J (Philipot et al. 2023). Our GaiaPMEX map for HD 28254, combining the constraints from ruwe (1.51; $5.2-\sigma$) and PMA (0.18 ± 0.04 mas yr $^{-1}$; $2.4-\sigma$), predicts a $>6-M_J$ companion with an sma of <4 au with 95.4% confidence. At 2.15 au, GaiaPMEX predicts a mass of within 6–30 M_J with 95.4% confidence and 9–15 M_J with 68.3% confidence. This is only marginally compatible with the results of Philipot et al. (2023), but their posterior distribution on the companion mass had a long tail toward larger mass. This indicates that the constraint from ruwe leads to an even higher mass for HD 28254 b.

HD 62364 (# 30). This F7V star located at 53 pc is known to host one RV companion of $M \sin i=12.7\pm 0.2$ M_J and $sma=6.15\pm 0.04$ au but constrained from HIPPARCOS–*Gaia* astrometry to a higher BD mass of 18.77 ± 0.66 M_J (Frensch et al. 2023). Our GaiaPMEX map for HD 62364, combining the constraints from ruwe (1.46; $5-\sigma$) and PMA (0.79 ± 0.03 mas yr $^{-1}$; $>9-\sigma$), predicts a 15–200 M_J companion with an sma of within 2–20 au with 95.4% confidence. This agrees at $2-\sigma$ with the published parameters for HD 62364 b.

HD 81040 (# 56). As already discussed in Paper I, for this 7.2 mag G2/3V star at 33 pc, the combination of PMA (0.15 ± 0.05 mas yr $^{-1}$; $1.5-\sigma$) and ruwe (1.60; $6.8-\sigma$) led GaiaPMEX to infer a companion with a mass of possibly as low as 6 M_J with an sma smaller than 4 au at 95.4% confidence. This was in good agreement with the known companion of HD 81040 at 1.94 au, first discovered as an 6.9 M_J super-Jupiter by Sozzetti et al. (2006), and further confirmed at a mass of $8.04^{+0.66}_{-0.54}$ M_J combining RVs and *Gaia* orbit fit of the astrometric time series (Gaia Collaboration et al. 2023a)⁷.

HD 9446 (# 100). This G5V star located at 53 pc is known to host two RV planets (Hébrard et al. 2010), with 0.7 ± 0.06 M_J

at 0.189 ± 0.006 au, and 1.82 ± 0.17 M_J at 0.654 ± 0.022 au. Our GaiaPMEX map for HD 9446, combining the constraints from ruwe (1.22; $2.8-\sigma$) and PMA (0.11 ± 0.05 mas yr $^{-1}$; $1.1-\sigma$), predicts a $>1.5-M_J$ companion within 7 au from the star with 95.4% confidence. It moreover predicts a mass of greater than 8 M_J in this $2-\sigma$ confidence region, for at least one of the two planet candidates. This would imply a system close to face on, with an inclination of $<15^\circ$. With an insignificant PMA, this result is mainly driven by the ruwe=1.22, which corresponds to $\alpha_{UEVA,ruwe}=0.12$ mas with $2.8-\sigma$ significance. Our analysis does not account for the presence of two planets. This situation will be explored in future studies.

USco 1621 A (# 6250). This young (5–10 Myr) Upper Scorpius M2.5 star is known to host a very wide substellar companion with a mass of 15 ± 2 M_J at a projected separation of 2880 ± 20 au detected by direct imaging (Chinchilla et al. 2020). The ruwe=1.176 of this source has a significance of $3.3-\sigma$. Our GaiaPMEX map for USco 1621 A using the constraints from ruwe predicts a $>5M_J$ companion within 10 au of the star with 95.4% confidence. The very wide companion is located beyond the 99.7% confidence region, predicting a ruwe of smaller than 1.176. The *Gaia* astrometry thus indicates the presence of a supplementary companion at smaller separation. As in the case of 2M0437 discussed above however, in such a young system one may expect significant accretion, which might induce astrometric jitter.

Transiting systems. We find six systems with transiting planets only, namely K2-123 (Livingston et al. 2018a) or # 5975, K2-153 (Livingston et al. 2018b) or # 6669, K2-174 (Barros et al. 2016; Livingston et al. 2019) or # 1933, K2-321 (Castro González et al. 2020) or # 2832, Kepler-125 (2 planets; Rowe et al. 2014) or # 8550, and TOI-261 (Hord et al. 2024) or # 331. In all those systems, the planets are located within 0.1 au and in the Neptunian regime in terms of radius, and thus also in terms of mass if applying a mass–radius relationship. However, our GaiaPMEX maps, with the constraints from ruwe (1.25; $3.1-\sigma$) and PMA (0.087 ± 0.053 mas yr $^{-1}$; $0.9-\sigma$) for TOI-261, predicts a mass of greater than 5 M_J and at $sma<20$ au (<3 au for TOI-261) with 95.4% confidence. In those systems, the *Gaia* astrometry shows that additional companions exist at larger orbital periods.

4.3. A focus on planet candidate hosts observed with HIPPARCOS

We found 259 sources in our sample that also have a HIPPARCOS identifier. We used GaiaPMEX on all the HIPPARCOS–*Gaia* (HG) data of those 259 sources and found 132 sources with a proper motion astrometric signature, α_{PMA} , more significant than $3-\sigma$. We identified 20 sources with an HG astrometry that could be compatible with a planet companion, and 51 sources possibly compatible with a BD companion. For the other 62 sources, GaiaPMEX predicts the existence of stellar companions.

Among the 20 planet candidate hosts, we find 5 planet systems that were already discussed in Sect. 4.2: HD 136118, HD 111232, HD 164604, HD 175167, and HD 23596. We find 9 spectroscopic binaries, including 7 SB1s, namely HD 75767, HD 17382, HD 108510, HD 112099, HD 2085, HD 23308, and HD 221818, and 2 SB2s, HD 30957 and BD+05 3080. Among the remaining 8 systems, there is 1 system with a known planet or BD companion, HD 40503, 1 candidate planetary system, HD 33636, 2 wide visual binary systems, HD 187129 and

⁷ See also the dedicated webpage on the *Gaia* ESA website at https://www.cosmos.esa.int/web/gaia/iow_20220131

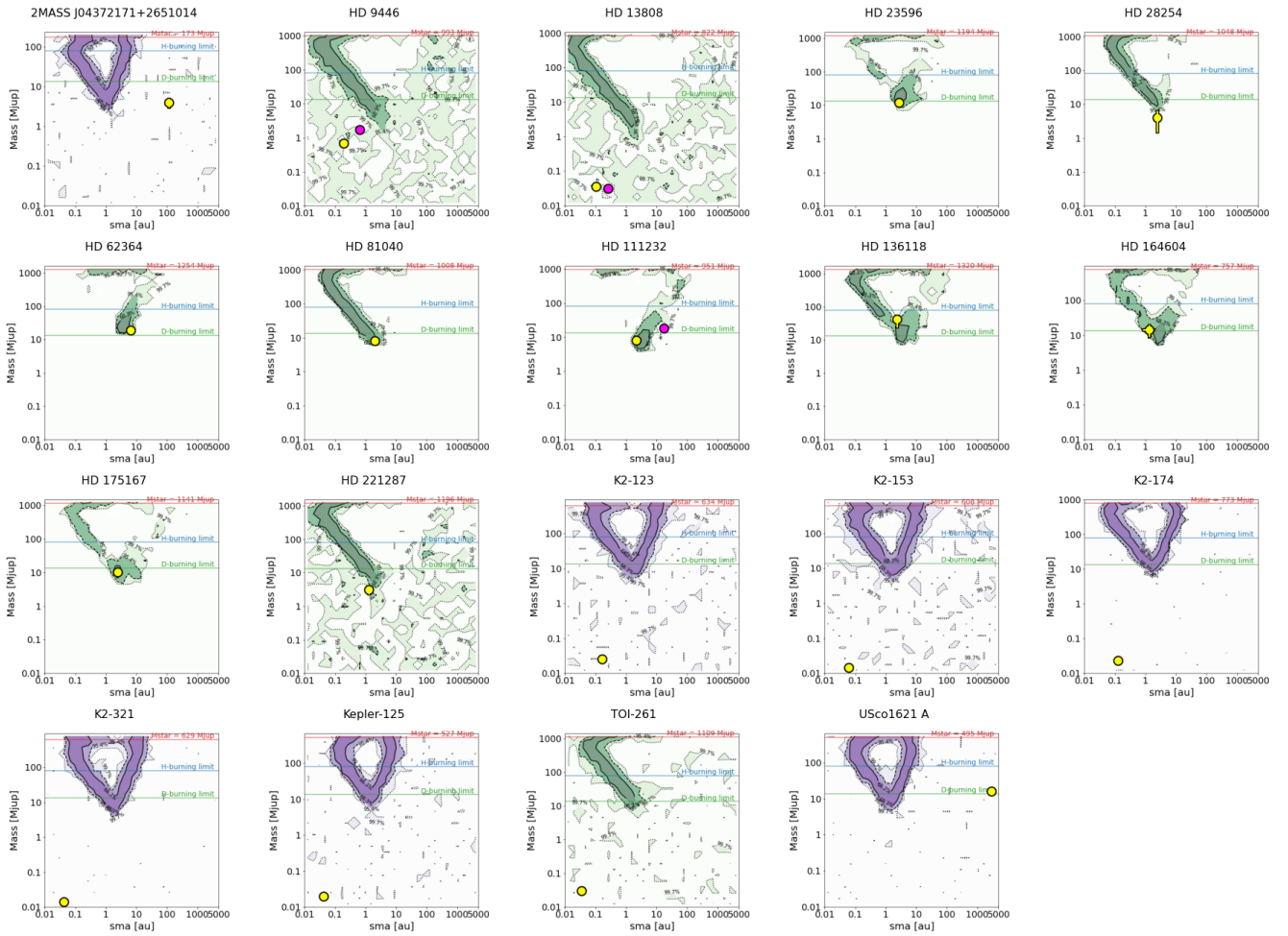


Fig. 11. PMEX maps for the NEA cross-matched sample, combining, when possible, the constraints from ruwe and PMa (green) or only ruwe (purple). The different shades of colour in each map are explained in Fig. 1.

HD 81697, and 2 systems with no known companions, CD-42 883 and HD 105330. We discuss these eight cases below.

HD 40503 (# 212). This source is a K2/3V star located at 25.5 pc. The astrometric orbit of HD 40503 was characterized by Holl et al. (2023) and Gaia Collaboration et al. (2023a), and was compared with the fit of publicly available RV by Marcussen & Albrecht (2023). Discrepant solutions were found: the RV implies a mass of $1.55 M_J$ on an edge-on orbit with a period of 758 days, while astrometry implies a mass of $5.18 \pm 0.59 M_J$ on an edge-on orbit with a period of 826 ± 50 days. Figure 12 shows the GaiaPMEX confidence region of the mass and sma of the companion derived from the combination of ruwe (1.41 ; $4.2\text{-}\sigma$) and PMa ($0.41 \pm 0.03 \text{ mas yr}^{-1}$; $>9\text{-}\sigma$). Excluding the equal-mass binary scenario, the 68.3% confidence region confirms that HD 40503 b could be a planet with a sma of 1.5–5 au and a higher mass within 4–13.5 M_J . Our analysis of the five-parameter model residuals thus indicate that HD 40503 b must have a face-on orbit with an inclination of $<3^\circ$.

HD 33636 (# 17). This G0V star located at 29 pc is known to host a planet candidate discovered by RV (Perrier et al. 2003) and characterized with an $M \sin i = 9.28 \pm 0.77 M_J$ and sma of 3.27 ± 0.19 au (Butler et al. 2006). An analysis of the absolute astrometry of HD 33636 using the Hubble Fine Guidance Sensor (HST-FGS), however, showed that the astrometric motion was rather compatible with a low-mass star with a mass of $142 M_J$.

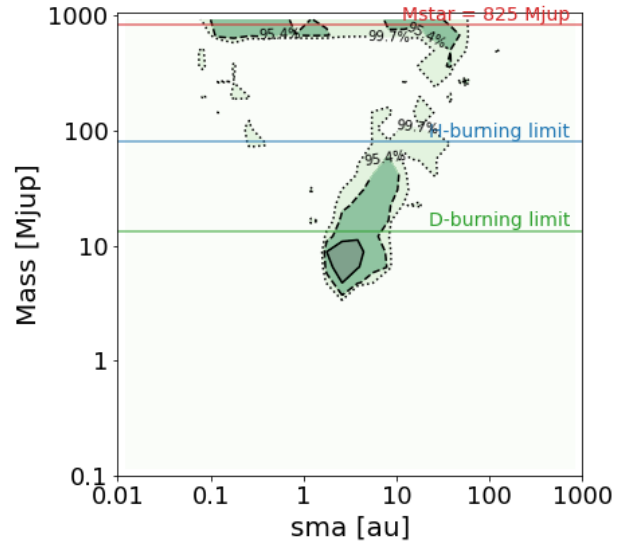


Fig. 12. GaiaPMEX maps for HD 40503 based on the combination of constraints from PMa and ruwe. Individual maps deduced from either PMa or ruwe are shown in Fig. E.1.

Figure 13 shows the GaiaPMEX confidence region on the mass and sma of the companion derived from the combination of

ruwe (1.88 ; $7.8\text{-}\sigma$) and PMa ($0.34\pm 0.04 \text{ mas yr}^{-1}$; $4.9\text{-}\sigma$). The 95.4% confidence region predicts a mass of greater than $7 M_J$ and an sma of smaller than 5 au. Most importantly, at the location of the known companion, at about 3.3 au, the GaiaPMEX map excludes the possibility of a companion with a mass of greater than $40 M_J$. This is, surprisingly, in total opposition to the result obtained from the HST-FGS astrometry. This is apparent in the individual maps obtained from considering either ruwe or PMa . Xiao et al. (2023) already noted an inconsistency and proposed a smaller mass of $77.8^{+6.9}_{-6.6} M_J$ based on the combination of the RV and the HG proper motion astrometry. Here, combining with the constraints from ruwe , we find a mass interval that is even lower and rather compatible with the initial value from Butler et al. (2006). Moreover, the value of the acceleration of HD 33636 measured by *Gaia* is published in the *Gaia*-NSS catalog, leading to $\gamma=1.8 \text{ mas yr}^{-2}$. Given that $\varpi=34 \text{ mas}$ and an sma of 3.3 au, we find that the star must be pulled by a companion of $\sim 15.4 M_J$. HD 33636 b is thus a substellar companion at the planet–BD limit.

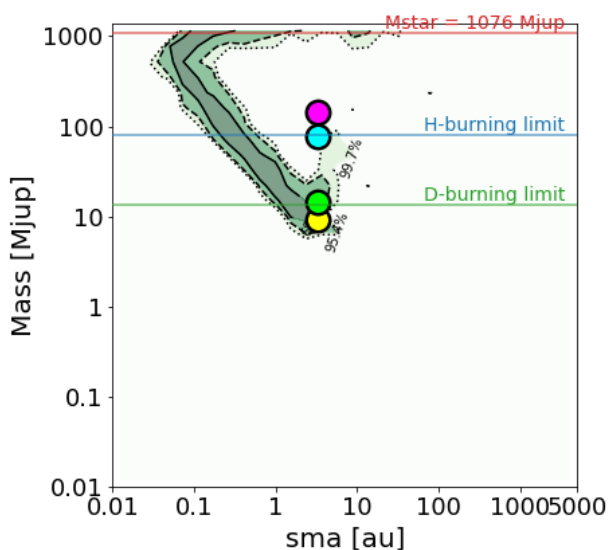


Fig. 13. Same as Fig. 12 but for HD 33636. We added the four possible solutions: from RV only (yellow), RV+FGS (magenta), RV+HG (cyan), and GDR3 acceleration (green).

HD 187129 (# 224). This very wide visual binary system, also known as WDS 19479+1002, and located at 100 pc, is composed of two stars separated by $\sim 50''$ ($\sim 5050 \text{ au}$) with a magnitude difference in the optical of $\Delta V=1.47$ (Mason et al. 2024). Our GaiaPMEX map for HD 187129, shown in Fig. 14, combining the constraints from ruwe (1.20 ; $2.9\text{-}\sigma$) and PMa ($0.21\pm 0.03 \text{ mas yr}^{-1}$; $4\text{-}\sigma$) predicts a $>4 M_J$ companion with an $\text{sma}<100 \text{ au}$ with 95.4% confidence. The main branch of the solution is located below 10 au, with a smaller 68.3% confidence region within 2–4 au and 8–30 M_J , but other solutions at lower/larger sma and larger mass cannot be excluded with sufficient confidence.

HD 81697 (# 205). This wide visual binary system, also known as WDS 09247-6055, and located at 67 pc, is composed of two stars separated by $\sim 1.5''$ ($\sim 100 \text{ au}$) with a magnitude difference in the optical of $\Delta V=2.96$ (Mason et al. 2024). Our GaiaPMEX map for HD 81697, shown in Fig. 14, combining the constraints from ruwe (1.42 ; $4.2\text{-}\sigma$) and PMa ($0.34\pm 0.07 \text{ mas yr}^{-1}$; $4.4\text{-}\sigma$),

predicts a $>6 M_J$ companion with an sma of $<10 \text{ au}$ with 95.4% confidence. The 68.3% confidence region is scattered but mainly centered within 1.5–6 au and 8–30 M_J . Other solutions at lower and larger sma and larger mass, including the stellar companion at 100 au, cannot be excluded with sufficient confidence.

CD-42 883 (# 422). This star has a mass of $0.89 M_\odot$ and is thus possibly of G8 spectral type. To our knowledge, it is not a known binary or a planetary system. Combining the constraints from ruwe (1.23 ; $3.3\text{-}\sigma$) and PMa ($0.48\pm 0.04 \text{ mas yr}^{-1}$; $>9\text{-}\sigma$), the GaiaPMEX map for this source, shown in Fig. 14, predicts at 95.4% confidence that CD-42 883 has a companion of $>10 M_J$ at $\text{sma}>2 \text{ au}$.

HD 105330 (# 12). This F8V star is known to show RV variability (Nordström et al. 2004) but no orbit was ever determined for the possible companion in this system. Combining the constraints from ruwe (2.09 ; $>9\text{-}\sigma$) and PMa ($0.51\pm 0.03 \text{ mas yr}^{-1}$; $7.2\text{-}\sigma$), the GaiaPMEX map for this source, shown in Fig. 14, predicts at 95.4% confidence that HD 105330 has a companion of $>7 M_J$ at $\text{sma}<10 \text{ au}$.

In summary, we confirm five planets (or low-mass BD) and find four new planet-candidate systems, HD 187129, HD 81697, CD-42 883, and HD 105330. Among the subset of HIPPARCOS sources with a α_{PMa} more significant than $3\text{-}\sigma$ in our catalog, we find $\sim 39\%$ to be BD (or stellar) companions, $\sim 46\%$ to be binary stars, and 3.7–6.8% to be planets. Extrapolating these percentages to our whole catalog suggests that most of the 9,698 systems that we identified do not contain planets, but rather BDs or stars. However, this extrapolation might not be permitted. For the HIPPARCOS sources for which both ruwe and PMa are significant, the GaiaPMEX map only leads to a $1\text{-}\sigma$ confidence region upon the planetary companion at 1–3 au when the individual maps from ruwe and PMa almost fully overlap. Most values of PMa would predict a larger mass for the companion at 1–3 au and lead to $1\text{-}\sigma$ confidence regions in the BD or stellar domain. Thus, the HIPPARCOS subsample might be strongly biased towards finding BDs or stellar companions. This implies that 3.7% is a minimum planet rate among our catalog of 9,698 systems.

5. Conclusion

In Paper I, we introduced GaiaPMEX, a tool that allows the characterization of the possible mass and sma of companions to stars observed with *Gaia* using the proper motion anomaly (PMa), the renormalized unit weight error (ruwe), and the astrometric excess noise (AEN). GaiaPMEX determines their significance within the null hypothesis that the star is single, and then models them based on the star’s reflex motion due to a companion, providing ranges of possible mass and sma . As mentioned in Sect. 2, the astrometric signature that is obtained from either the ruwe or the AEN allows the determination of the minimum mass of a companion around any source of the GDR3 database brighter than $G=16$.

In this work, we report an extensive catalog of 9,698 planet-candidate hosts with a primary star more massive than $0.5 M_\odot$ in which the astrometric signature of ruwe , $\alpha_{\text{UEVA,ruwe}}$, is more significant than $2.7\text{-}\sigma$, predicting a minimum mass of a companion lying in the planetary domain, that is $<13.5 M_J$. Given the mass– sma degeneracy, many of these systems could actually be binaries, although a cross-match with existing catalogs of exoplanets and validated astrometric orbital solutions allowed us to

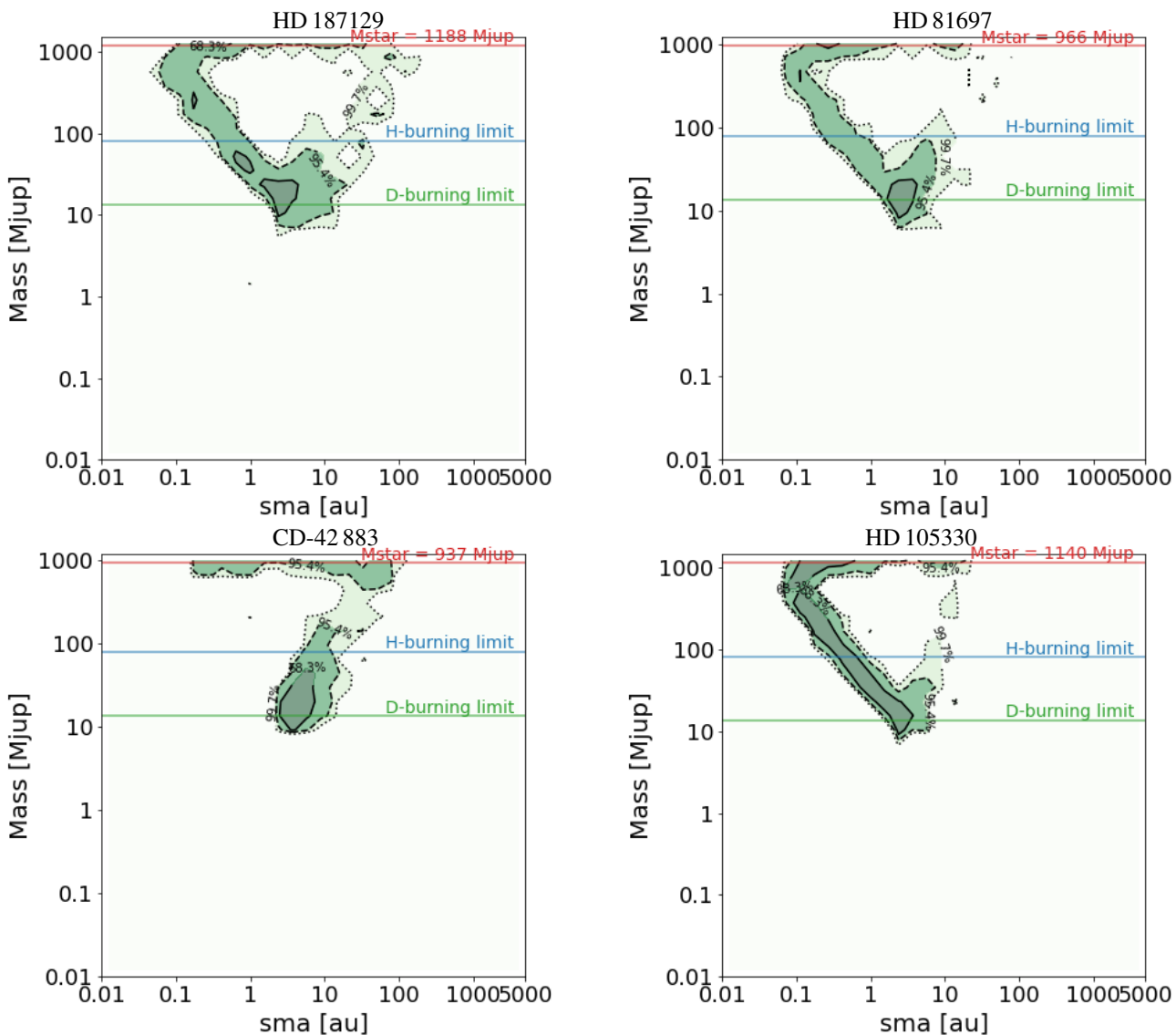


Fig. 14. Same as Fig. 12 but for HD 187129 (top-left), HD 81697 (top-right), CD-42883 (bottomn-left), and HD 105330 (bottom-right).

confirm the planetary nature of some of our identified companions. A cross-check with the *Gaia*-NSS shows that our source selection process is approximately eight times more efficient at selecting planets than it is at selecting BD companions or binary stars in the domain of sensitivity of *Gaia*. Of the 260 systems observed with HIPPARCOS, focusing on the 134 systems that have a PMA significance larger than $3-\sigma$, we find that 5–9 of them (3.7–6.7%) are likely detected planets. This could suggest that, nonetheless, at best $\sim 7\%$ of the sources of our catalog are truly planetary. However, this number was found using systems with a PMA measurement, which favors binaries, unless both PMA and ruwe coincide on predicting a planet companion at about 1–3 au. A systematic vetting of this catalog will be carried out in future studies in order to determine the true frequency of binaries and planets in our sample of 9,698 sources.

Finally, as shown in Paper I, *Gaia*'s sensitivity is optimum for the detection of planets down to $\sim 0.1 M_J$ around nearby (< 10 pc) low-mass ($< 0.5 M_\odot$) stars. We thus plan to extend this

catalog to *M*-dwarfs with $M_\star < 0.5 M_\odot$ and $G > 16$, which were excluded from the present version of the catalog.

Data availability

Appendices D–F are available at the following link at <https://zenodo.org>. Table B.1 is only available in electronic form at the CDS via anonymous ftp to cdsarc.u-strasbg.fr (130.79.128.5) or via <http://cdsweb.u-strasbg.fr/cgi-bin/qcat?J/A+A/>.

Acknowledgements. We are very thankful to the anonymous referee for her/his thorough and courageous reading that led to significant improvements of this article. We thank D. Ségransan for fruitful discussions. This work has made use of data from the European Space Agency (ESA) mission *Gaia* (<https://www.cosmos.esa.int/gaia>), processed by the *Gaia* Data Processing and Analysis Consortium (DPAC, <https://www.cosmos.esa.int/web/gaia/dpac/consortium>). Funding for the DPAC has been provided by national institutions, in particular the institutions participating in the *Gaia* Multilateral Agreement. This work was granted access to the HPC resources of MesoPSL financed by the Region Ile de France and the project EquipMeso (reference ANR-10-EQPX-29-01) of the programme Investissements d'Avenir supervised by the Agence

Nationale pour la Recherche. This project has received funding from the European Research Council (ERC) under the European Union's Horizon 2020 research and innovation programme (COBREX; grant agreement n° 885593). F.K. acknowledges funding from the initiative de recherches interdisciplinaires et stratégiques (IRIS) of Université PSL "Origines et Conditions d'Apparition de la Vie (OCAV)", as well as from the Action Pluriannuelle Incitative Exoplanètes from the Observatoire de Paris - Université PSL. F.K. also acknowledges funding from the American University of Paris.

References

- Ahrer, E., Queloz, D., Rajpaul, V. M., et al. 2021, *MNRAS*, 503, 1248
- Arriagada, P., Butler, R. P., Minniti, D., et al. 2010, *ApJ*, 711, 1229
- Barros, S. C. C., Demangeon, O., & Deleuil, M. 2016, *A&A*, 594, A100
- Brandt, T. D. 2021, *ApJS*, 254, 42
- Butler, R. P., Wright, J. T., Marcy, G. W., et al. 2006, *ApJ*, 646, 505
- Canal, L. 2005, *Computational Statistics & Data Analysis*, 48, 803
- Castro González, A., Díez Alonso, E., Menéndez Blanco, J., et al. 2020, *MNRAS*, 499, 5416
- Chinchilla, P., Béjar, V. J. S., Lodieu, N., et al. 2020, *A&A*, 633, A152
- De Rosa, R. J., Nielsen, E. L., Wahhaj, Z., et al. 2023, *A&A*, 672, A94
- Fabrizius, C., Luri, X., Arenou, F., et al. 2021, *A&A*, 649, A5
- Feng, F., Butler, R. P., Vogt, S. S., et al. 2022, *ApJS*, 262, 21
- Fischer, D. A., Marcy, G. W., Butler, R. P., et al. 2002, *PASP*, 114, 529
- Franson, K., Bowler, B. P., Zhou, Y., et al. 2023, *ApJ*, 950, L19
- Frensch, Y. G. C., Lo Curto, G., Bouchy, F., et al. 2023, *A&A*, 675, A173
- Gaia Collaboration, Arenou, F., Babusiaux, C., et al. 2023a, *A&A*, 674, A34
- Gaia Collaboration, Brown, A. G. A., Vallenari, A., et al. 2021, *A&A*, 649, A1
- Gaia Collaboration, Creevey, O. L., Sarro, L. M., et al. 2023b, *A&A*, 674, A39
- Gaidos, E., Hirano, T., Kraus, A. L., et al. 2022, *MNRAS*, 512, 583
- Gan, T. 2023, *Research Notes of the American Astronomical Society*, 7, 226
- Hébrard, G., Bonfils, X., Ségransan, D., et al. 2010, *A&A*, 513, A69
- Holl, B., Perryman, M., Lindegren, L., Segransan, D., & Raimbault, M. 2022, *A&A*, 661, A151
- Holl, B., Sozzetti, A., Sahlmann, J., et al. 2023, *A&A*, 674, A10
- Hord, B. J., Kempton, E. M. R., Evans-Soma, T. M., et al. 2024, *AJ*, 167, 233
- Kane, S. R. 2013, *ApJ*, 766, 10
- Kervella, P., Arenou, F., Mignard, F., & Thévenin, F. 2019, *A&A*, 623, A72
- Kervella, P., Arenou, F., & Thévenin, F. 2022, *A&A*, 657, A7
- Kiefer, F. 2019, *A&A*, 632, L9
- Kiefer, F., Hébrard, G., Lecavelier des Etangs, A., et al. 2021, *A&A*, 645, A7
- Kiefer, F., Hébrard, G., Sahlmann, J., et al. 2019, *A&A*, 631, A125
- Lindegren, L., Hernández, J., Bombrun, A., et al. 2018, *A&A*, 616, A2
- Lindegren, L., Klioner, S. A., Hernández, J., et al. 2021, *A&A*, 649, A2
- Livingston, J. H., Crossfield, I. J. M., Petigura, E. A., et al. 2018a, *AJ*, 156, 277
- Livingston, J. H., Crossfield, I. J. M., Werner, M. W., et al. 2019, *AJ*, 157, 102
- Livingston, J. H., Endl, M., Dai, F., et al. 2018b, *AJ*, 156, 78
- Marcussen, M. L. & Albrecht, S. H. 2023, *AJ*, 165, 266
- Martoli, E., McArthur, B. E., Benedict, G. F., et al. 2010, *ApJ*, 708, 625
- Mason, B. D., Wycoff, G. L., Hartkopf, W. I., Douglass, G. G., & Worley, C. E. 2001, *AJ*, 122, 3466
- Mason, B. D., Wycoff, G. L., Hartkopf, W. I., Douglass, G. G., & Worley, C. E. 2024, *VizieR Online Data Catalog: The Washington Visual Double Star Catalog (Mason+ 2001-2020)*, *VizieR On-line Data Catalog: B/wds*. Originally published in: 2001AJ....122.3466M
- Mayor, M., Marmier, M., Lovis, C., et al. 2011, *arXiv e-prints*, arXiv:1109.2497
- Mayor, M., Udry, S., Naef, D., et al. 2004, *A&A*, 415, 391
- Mesa, D., Gratton, R., Kervella, P., et al. 2023, *A&A*, 672, A93
- Naef, D., Mayor, M., Benz, W., et al. 2007, *A&A*, 470, 721
- Naef, D., Mayor, M., Lo Curto, G., et al. 2010, *A&A*, 523, A15
- Nordström, B., Mayor, M., Andersen, J., et al. 2004, *A&A*, 418, 989
- Perrier, C., Sivan, J. P., Naef, D., et al. 2003, *A&A*, 410, 1039
- Perryman, M., Hartman, J., Bakos, G. Á., & Lindegren, L. 2014, *ApJ*, 797, 14
- Philipot, F., Lagrange, A. M., Kiefer, F., et al. 2023, *A&A*, 678, A107
- Rowe, J. F., Bryson, S. T., Marcy, G. W., et al. 2014, *ApJ*, 784, 45
- Sahlmann, J., TriAUD, A. H. M. J., & Martin, D. V. 2015, *MNRAS*, 447, 287
- Sozzetti, A., Pinamonti, M., Damasso, M., et al. 2023, *A&A*, 677, L15
- Sozzetti, A., Udry, S., Zucker, S., et al. 2006, *A&A*, 449, 417
- Wilson, E. B. & Hilferty, M. M. 1931, *Proceedings of the National Academy of Science*, 17, 684
- Winn, J. N. 2022, *AJ*, 164, 196
- Xiao, G.-Y., Liu, Y.-J., Teng, H.-Y., et al. 2023, *Research in Astronomy and Astrophysics*, 23, 055022

Appendix A: Table of acronyms used in the text with their definitions and page references.

Notation	Description	Page List
5p	5-parameters	3–5, 8
6p	6-parameters	3–5, 8
AEN	astrometric excess noise	2, 11
AL	along scan	2
BD	brown dwarf	1, 7, 9, 11, 12
CDS	Centre de Données de Strasbourg	5
CU8	Coordination unit 8	3, 4
FoV	field of view	2
FP	false-positives	4, 7
<i>Gaia</i> -NSS	<i>Gaia</i> DR3 non single star catalog	1, 5–7, 11, 12, 15, 16
<i>Gaia</i> PMEX	<i>Gaia</i> DR3 proper motion anomaly and astrometric noise excess	1–4, 7–11, 15
GDR3	third <i>Gaia</i> data release	1–4, 6, 8, 11, 15
GDR4	fourth <i>Gaia</i> data release	7, 8
HG	HIPPARCOS– <i>Gaia</i>	9, 11
IPD	Image parameter determination	3
NEA	NASA Exoplanet Archive	1, 6, 8
PMa	proper motion anomaly	1, 2, 6–12
PSF	point spread function	3
RA	right ascension	2, 4
ruwe	renormalised unit weight error	1–12, 15
RV	radial velocity	1, 7–11
sma	semi-major axis relative to the central star	1–3, 5, 8, 9, 11, 16
UEVA	unbiased estimator of variance a posteriori	2–9, 11, 16

Appendix B: Catalog of candidate systems with exoplanet

Table B.1. Extract of the full table of candidate systems with the systems discussed in Sects. 4.2 and 4.3.

Identifiers	<i>Gaia</i> DR3 ID	main alias	HIP alias	<i>G</i>	Fluxes σ_V	$\sigma_B - V$	Colors $BP - RP$	σ_{π} (mas)	Stellar properties $\sigma_{\text{sp}} \text{ type}$	M_{star} (M_{\odot})	σ_{dataset} Sp/Ep	b_{NebV}	b_{NebI}	b_{NebJ}	b_{AEN} (mas)	b_{ruwe}	Noise estimations σ_{ruwe} (mas)	σ_{ruwe} (mas)	σ_{ruwe} (mas)	Astrometric signatures f_{ruwe}	f_{ruwe}	Astrometric signatures P_{ruwe}	Planet candidate properties σ_{ruwe} (M_{Jup})	σ_{ruwe} (M_{Jup})	Planet candidate properties σ_{ruwe} (M_{Jup})	Binary and planet crossmatch <i>Gaia</i> -NSS (0/1)	WDS alias	NEA N_{NEA}
12	347264093895300096	HD 105330	HIP 59135	6.59	6.73	5.30	0.510	0.76	F8V	1.088	Sp	51	0.363	2.087	0.164	0.049	0.077	0.035	0.00000	>9	12.2	2.16	65.83	0	0			0
16	4415515934099120768	HD 136118	HIP 74948	6.81	6.94	5.60	0.520	0.690	F7V	1.260	Sp	23	0.221	1.431	0.159	0.056	0.070	0.163	0.00164	3.1	11.1	2.27	44.94	0	1			0
17	3238810137558836352	HD 33636	HIP 24205	6.86	7.12	5.87	0.610	0.750	G0V, CH-0.3	1.027	Sp	40	0.297	1.881	0.157	0.058	0.073	0.252	0.00000	7.5	8.7	2.12	71.61	0	1			0
29	224870885460640016	HD 23596	HIP 17747	7.12	7.24	6.00	0.530	0.689	F8	1.098	Sp	42	0.237	1.345	0.158	0.068	0.072	0.142	0.00071	3.4	9.0	2.17	41.87	0	1		WDS J03480+4032A	0
30	521420956293214208	HD 62364	HIP 36941	7.20	7.31	6.00	0.680	0.879	F7V	1.197	Sp	35	0.237	1.461	0.158	0.070	0.080	0.193	0.00000	4.8	13.2	2.23	42.10	0	2			0
42	5855730384310531200	HD 111232	HIP 62534	7.42	7.61	5.90	0.755	0.889	G8VFC-1.0	0.897	Sp	45	0.209	1.244	0.152	0.080	0.081	0.140	0.00036	3.6	4.3	2.03	70.09	0	1			0
6	4781533628545774656	HD 28254	HIP 20066	7.51	7.68	6.01	0.676	0.844	G5V	1.000	Sp	32	0.235	1.509	0.152	0.083	0.077	0.193	0.00000	5.0	12.3	2.10	38.06	0	1		WDS J04248+5037A	0
6	4781533628545774656	HD 28254	HIP 20066	7.51	7.68	6.01	0.676	0.844	G5V	1.000	Sp	32	0.235	1.509	0.152	0.083	0.077	0.193	0.00000	5.0	12.3	2.10	38.06	0	1			0
66	6989603813690967808	HD 221287	HIP 14084	7.69	7.81	6.29	0.663	0.864	F7V	1.142	Sp	58	0.157	1.223	0.165	0.088	0.074	0.123	0.00276	3.0	8.7	2.20	39.23	0	1			0
74	642118739093252224	HD 175167	HIP 93281	7.84	8.00	6.29	0.780	0.900	G5V/IV	1.089	Sp	73	0.181	1.173	0.150	0.092	0.074	0.108	0.00312	3.0	9.4	2.16	30.34	0	1			0
89	4743692151804240896	HD 13808	HIP 10301	8.12	8.38	6.25	0.852	1.059	K2V	0.785	Sp	42	0.133	1.169	0.147	0.089	0.079	0.119	0.00487	2.8	3.3	1.94	68.82	0	2			0
100	302956655074266112	HD 9446	HIP 7245	8.22	8.46	7.28	0.330	0.925	G5V	0.948	Sp	39	0.200	1.418	0.120	0.044	0.078	0.118	0.00639	2.7	6.6	2.06	41.09	0	2			0
205	5299152644351701760	HD 81697	HIP 46151	8.97	9.21	7.03	0.990	1.124	G8/K1	0.922	Sp	30	0.157	1.408	0.116	0.040	0.076	0.122	0.00004	4.1	10.0	2.04	30.74	0	0		WDS J09247+6055AB	0
212	2884087104955208064	HD 40503	HIP 28193	8.97	9.12	7.91	0.550	0.671	K2/IV	0.788	Sp	39	0.155	1.202	0.122	0.041	0.080	0.100	0.00494	2.8	12.7	2.19	21.71	0	0			0
224	430196366405443328	HD 18729	HIP 97410	9.05	9.12	7.91	0.550	0.671	G0	1.134	Sp	39	0.155	1.202	0.122	0.041	0.080	0.100	0.00494	2.8	12.7	2.19	21.71	0	0			0
302	40624601648807168	HD 164604	HIP 88414	9.33	9.83	8.18	1.050	1.268	K3.5V:K	0.745	Sp	28	0.177	1.158	0.110	0.032	0.128	0.174	0.00000	6.2	6.6	1.90	47.57	0	1			0
421	24038336253476768	TOI 1452	HIP 12369	9.48	9.79	8.18	0.529	0.722	F8/G0V	1.099	Sp	57	0.124	1.231	0.119	0.036	0.175	0.00033	3.0	7.4	2.14	36.84	0	1			0	
431	24038336253476768	TOI 1452	HIP 12369	9.48	9.79	8.18	0.529	0.722	F8/G0V	1.099	Sp	57	0.124	1.231	0.119	0.036	0.175	0.00033	3.0	7.4	2.14	36.84	0	1			0	
432	24038336253476768	TOI 1452	HIP 12369	9.48	9.79	8.18	0.529	0.722	F8/G0V	1.099	Sp	57	0.124	1.231	0.119	0.036	0.175	0.00033	3.0	7.4	2.14	36.84	0	1			0	
1933	4621766333148416	K2-174	HIP 12368	12.00	9.94	9.50	0.740	1.482	K7V	0.738	Sp	56	0.106	1.430	0.105	0.019	0.073	0.094	0.00337	3.6	8.6	1.90	18.94	0	0			0
2832	385644962754492392	K2-321		12.81			2.141	12.99	K7V	0.600	Sp	25	0.150	1.466	0.111	0.054	0.076	0.123	0.00024	3.7	7.8	1.77	23.01	0	1			0
5975	68506515507248192	K2-123		14.08			11.06	1.905	M0V	0.605	Sp	57	0.025	1.111	0.073	0.118	0.077	0.066	0.00321	2.9	8.9	1.78	10.96	0	1			0
6250	60486080690968960	USco 1621 A		14.15			10.19	2.676	M2.5e	0.660	Sp	50	0.073	1.176	0.079	0.120	0.075	0.078	0.00088	3.3	9.2	1.83	13.49	0	1			0
6669	3700937760929835648	K2-153		14.25			1.454	1.960	M3.0V	0.580	Sp	31	0.066	1.135	0.073	0.128	0.076	0.078	0.00570	2.8	9.0	1.75	12.17	0	1			0
6883	151499478104075008	2MASS J04372171+26051014		14.31			10.39	2.860	M4	0.642	Sp	27	0.089	1.214	0.084	0.129	0.074	0.096	0.00195	3.1	10.5	1.81	14.14	0	1			0
8550	2086439488284337536	Kepler-125		14.75	14.61	11.68	0.471	1.971	M1V	0.599	Sp	41	0.052	1.108	0.074	0.074	0.077	0.087	0.00374	2.9	13.1	1.77	9.61	0	2			0

Notes.

(^a) Taken from Simbad. (^b) Taken from the GDR3. (^c) CU8 database stellar mass, or mass-Flame (see Sect. 3). (^d) N_{AL} is the average number of along-scan angle measurements. See paper I for details. (^e) Estimated from the GDR3 catalog. See paper I for details. (^f) $\sigma_{\text{UEVA,ruwe}}$ is the astrometric signature calculated with ruwe. P_{ruwe} is the confidence that σ_{UEVA} rejects the single-star hypothesis and s_{σ} is the corresponding significance expressed as $N \cdot \sigma$. (^g) Mass and sma of the inferred companion at the minimum of the GaiaPMEX ruwe curve. See paper I for details. (^h) The separation $\rho = \text{sma} \times \varpi$. (ⁱ) Flag=1 if an orbital or acceleration solution is found in the *Gaia*-NSS, 0 otherwise. (^j) Number of planets already detected in the system cross-matched from the NASA Exoplanet Catalog. The full catalog is available at the CDS

Appendix C: Details on the calculation of the predicted α_{UEVA} for the H23 sample

We used the Eq. 6 to calculate the α_{UEVA} given the semi-major axis of a star and its orbital period P . There are two possible equations, one for $P < 3$ yr, with α_{UEVA} directly proportional to the star's semi-major axis, and another for $P > 3$ yr, with α_{UEVA} proportional to the gravitational pull due to the companion. We used the semi-major axis of the photocenter divided by the parallax as an approximation of the semi-major axis of the primary star, a_* , if not found in the *Gaia*-NSS catalog. The primary star's semi-major axis is known whenever there was, on top of astrometry, radial velocity data coming from the RVS instrument on-board, and an SB1/SB2 solution to the RV variations determined.

Moreover, when the period is larger than 3 yrs, if M_* was known and fulfilled the C_3 requirement of Sect. 3, we used the literature period given in H23's table A.1 to calculate the sma and mass of the companion by solving the equation based on Kepler's third law:

$$\text{sma} = M_*^{1/3} (1 + q)^{1/3} \left(\frac{P}{\text{yr}} \right)^{2/3} \quad (\text{C.1})$$

with $q = M_c/M_*$ the mass ratio. This can be expressed as a cubic equation on $Q = 1/q$ since $\text{sma} = a_* (1 + Q)$:

$$Q^3 + 2Q^2 + Q - \frac{M_*}{a_*^3} \left(\frac{P}{\text{yr}} \right)^2 = 0 \quad (\text{C.2})$$

which has a single real root given by:

$$\begin{cases} a = 1 \\ b = 2 \\ c = 1 \\ d = -M_* a_*^{-3} P(\text{yr})^2 \end{cases}$$

$$\begin{cases} \Delta_0 = b^2 - 3ac \\ \Delta_1 = 2b^3 - 9abc + 27a^2d \end{cases}$$

$$C = \text{sign}(\Delta_1) \sqrt[3]{\frac{|\Delta_1| + \sqrt{\Delta_1^2 - 3\Delta_0^3}}{2}}$$

$$Q = -\frac{1}{3a} \left(b + C + \frac{\Delta_0}{C} \right) \quad (\text{C.3})$$

From Q and M_* we deduce M_c and from Eq. C.1 we find the relative sma of the companion to the primary star. The use of Eq. 6 is then straightforward to determine a prediction of α_{UEVA} . Uncertainties are obtained by bootstrap, accounting for all input parameters and their individual uncertainties. All quantities entering this computation are written explicitly for all the 202 sources of H23 with $G < 16$.